MINISTRY OF EDUCATION AND TRAINING

MINISTRY OF AGRICULTURE AND RURAL DEVELOPMENT

VIETNAM NATIONAL UNIVERSITY OF FORESTRY

BUI LE HONG TRUONG

RESEARCH ON DYNAMICS AND CONTROL OF LOG CARRIAGE IN AUTOMATIC WOOD SAWING LINES

DOCTORAL DISSERTATION SUMMARY

Major: Mechanical Engineering

Code: 9.52.01.03

Hanoi, 2025

The dissertation was completed at:

VIETNAM NATIONAL UNIVERSITY OF FORESTRY

Scientific Supervisors:

1. Dr. Tran Van Tuong

2. Dr. Pham Van Tinh

Reviewer 1:

Reviewer 2:

Reviewer 3:

The dissertation will be defended before the University-level Dissertation Committee at:
Vietnam National University of Forestry – Xuan Mai, Chuong My, Hanoi

At: time , Date month year 2025

The dissertation can be accessed at:The National Library of Vietnam, The Library of Vietnam National University of Forestry

LIST OF PUBLISHED ARTICLES OF THE THESIS

1- Son Hoang, TruongBui Le Hong, Anh Nguyen Pham Thuc, Tuong Tran Van , Tinh Pham Van, Trung Nguyen Van, (July 29th - 30th, 2022), "Research Design and Manufacture of Automatic Edging and Trimming System for Wood Board from Wagon in Sawing Line Using PLC Control System", *2022 6th International Conference on Green Technology and Sustainable Development (GTSD), Electronic ISBN:978-1-6654-6628-8, Print on Demand(PoD) ISBN:978-1-6654-6629-5.*

https://ieeexplore.ieee.org/xpl/conhome/9987719/proceeding

DOI: 10.5267/j.esm.2024.1.008

2- Hoang Son [a] , Vu Khac Bay [b] , Tran Van Tuong [a] , Bui Le Hong Truong [c] , Luong Anh Tuan [d*] and Hoang Hai Son [b] , "Horizontal oscillations of the wood sawing support during the cutting process in a wood sawing line using a vertical bandsaw", *Engineering Solid Mechanics* 12 (2024) 247-258. ISSN 2291-8752 (Online) - ISSN 2291-8744 (Print)

https://www.growingscience.com/esm/online/esm_2024_8.pdf

DOI: 10.1109/GTSD54989.2022.9989051

INTRODUCTION

1. Problem statement

From 2016 to 2018, the Ministry of Science and Technology assigned the Forestry University to preside over the national independent project "Research, design, and manufacture of automatic wood sawing equipment line with a capacity of 3 - 4 m3 / h of finished wood" code DTĐL.CN-10/16. The project designed and manufactured an automatic wood sawing line.

During the operation of the carriage system, there are many factors affecting the productivity of the production line, product quality and safety during the operation process, of which there are 3 main issues that need attention as follows:

Firstly, the cart and the heavy round wood are distributed to 3 pairs of wheels moving on two rails placed on a concrete floor. Because the load concentrated on the wheels is different and moving on two rails, in addition to the phenomenon of oscillation along the rail direction, the cart also has the phenomenon of oscillation horizontally.

Second, when an incident occurs, such as a broken saw blade, an obstacle is detected, or other dangerous situations occur that require the carriage to be controlled to stop immediately to ensure safety.

Third, to increase the productivity of the line, the moving speed of the carriage needs to be as high as possible while still ensuring safety, braking ability and sawing quality.

Based on the above issues, the thesis topic: " **Research on dynamics and control of carriages in automatic wood sawing lines** ", which mainly focuses on studying the dynamics of longitudinal movement related to the carriage's moving speed, the elastic parameters of the foundation and of the rails related to the carriage's lateral oscillation; at the same time, studying the carriage's braking ability to provide parameters in the details of the braking system and as input parameters in the braking control process.

2. Research purpose of the thesis

Build a model, establish dynamic equations and control the carriage during the automatic wood sawing process, survey the established equations to determine the parameters for constructing the carriage track foundation, and at the same time determine the braking force of the carriage when the carriage has an accident to improve the productivity and quality of the sawing circuit and safety of the automatic timber sawing carriage system.

3. New contributions of the thesis

1. The thesis has built a model, established the dynamic equation and the algorithm to control the motion of the carriage. The horizontal oscillation of the wood sawing plane has been calculated, the problem is converted to the oscillation of the beam on an elastic foundation, bearing many concentrated moving loads. By using the properties of the Dirac function, the thesis has established the horizontal oscillation equation of the sawing circuit and given the solution in analytical form. With the obtained expressions of the natural oscillation frequency and the forced oscillation frequency, it is possible to conclude: With the wood sawing chain systems using vertical band saws and automatic wood sawing carriages, the resonance phenomenon of the beam does not occur.

2. The thesis has investigated the horizontal oscillation equation of the sawn joint and given the results (Table 3.2), which shows the pairs of values of the bending stiffness of

the rail beam *EI* and the foundation coefficient $k = k_0.b$ corresponding to the maximum horizontal oscillation amplitude of the carriage. Based on this result, it is possible to make a reasonable choice of parameters of EI and k_0, serving the construction process when installing the carriage foundation. From the survey results, the parameters when constructing and installing the carriage are determined as follows: When $k_d = 8$ KN/m^3, concrete grade M300, concrete layer thickness $h_n = 0.88$ m. When $k_d = 14$ KN/m^3, concrete grade M300, concrete layer thickness $h_n = 0.7$ m.

3. The thesis has built a model, established the dynamic equation of the carriage braking process, the survey results of the dynamic equation of carriage braking determined the parameters for carriage braking as follows: The braking traction system must achieve a traction acceleration $a_k \geq 20$ m/s^2 and brake pulling force $F \geq 2683$ N, carriage brake pulling cable diameter $\Phi = 22$ mm .

4. Scientific significance of the thesis

Based on the theory of dynamics, the establishment of the horizontal oscillation equation of the saw blade is transferred to the problem of oscillation of the beam on the Winkler elastic foundation, subjected to many concentrated and moving loads. The survey results have determined the pairs of values of the bending stiffness of the rail EI and the foundation coefficient k, ensuring that the maximum horizontal oscillation amplitude of the saw blade is within the allowable limit, helping to choose the appropriate technical parameters for the installation of the saw blade system. These are scientific contributions and have reference value for studies on the dynamics of carriages in the saw blade chain using vertical band saws and for other similar research subjects.

5. Practical significance of the thesis

The research results of the thesis can be used as reference material for the process of calculating and designing automatic wood sawing carriages, and at the same time used for the installation and completion of carriages in the automatic wood sawing line under the national level project code DTĐL.CN-10/16, in order to improve the productivity of the line, improve the quality of sawn boards and ensure the safety of people and equipment when operating the line, this is the practical significance of the thesis.

CHAPTER 1 OVERVIEW OF THE RESEARCH PROBLEM

1.1 General overview of the wood carriage system in the automatic wood sawing line using vertical band saw

Using an automatic sawing system with a vertical band saw will bring advantages including improving productivity and quality of sawn boards, improving gas production rate, thereby reducing production costs, ensuring safety during the sawing process. However, using an automatic sawing system requires high initial investment costs, high requirements for operating techniques and maintenance. Therefore, automatic sawing systems are mainly used in large-scale production facilities, with the ability to invest and meet the requirements for operating techniques and maintenance.

1.2. Situation of using automatic wood sawing lines in the world and in Vietnam

1.2.1. Overview of the situation of using automatic wood sawing lines in the world

The research on technology and design of automatic wood sawing equipment production lines in the world has achieved great achievements, contributing to improving productivity, quality and finished product rate. However , automatic wood sawing equipment lines require large investment capital, complex usage techniques and depend on the wood objects of each country, each nation. When applied to each country, it is necessary to have research suitable for the wood objects that need to be sawn and the investment capital as well as the level of workers operating the equipment line [38], [37], [17], [13]

1.2.2. Overview of the situation of using automatic wood sawing lines in Vietnam

Currently in Vietnam there are about 5,000 wood processing establishments, of which 60% are small and medium-sized establishments mainly operating at the craft village and household scale, focusing on the production of handicrafts for the domestic market. The rest are large-scale wood processing factories producing wooden products mainly for export.

For small-scale facilities, to carry out the sawing process, people can now use some popular saws including horizontal band saws, circular saws, and circular saws.

Figure 1.6 1Circular saw used to cut round wood into boards.

Figure 1.6 is a circular saw, a type of vertical circular saw mainly used to cut wood boards with a diameter of less than 30 cm. When cutting, two people need to stand on both sides of the saw table to carry out the process of putting the wood in to cut and taking the board out.

In the South, some rubber wood processing companies in Binh Duong have used semi-automatic wood sawing lines, in which the wood feeding and pushing stages are by conveyor belt, sawing is by band saw, but the wood clamping system is still done manually. These wood sawing lines have higher productivity, reducing the workload for workers, but the product quality is not high, the gas conversion rate is low. Some processing factories in Quy Nhon - Binh Dinh also use improved band saws using carts to push the wood during the sawing process. The thickness of the sawn board is controlled by an electric motor, but the manual level is still high and the productivity is limited [9] .

Figure 1.8 shows a sample of a wood sawing line installed by SUMAC Machinery & Equipment Company. This equipment can saw wood with a diameter of Ø400 mm ÷ Ø1000 mm, a maximum tree length of up to 6 m with a cutting tolerance of ±1 mm. In addition, automatic conveyor systems support fast feeding of wood in combination with a PLC control system. However, the limitation of this line is that there is no automatic system to set up a sawing map to optimize the gas ratio [14]

Figure 1.8 2Automatic slitting line of SUMAC Machinery & Equipment Company

Thus, the current sawn timber production stage in Vietnam for small and medium-sized processing facilities is mainly carried out by vertical band saws and horizontal band saws using human power to push the wood manually, so productivity is low, labor costs are high, leading to low economic efficiency and lack of initiative in labor resources. Some facilities with large production scale and investment capacity have imported automatic and semi-automatic sawing lines to serve the sawn timber production stage. However, these lines are often expensive, difficult to care for, maintain, repair and replace, leading to limited economic efficiency and lack of initiative in handling technical problems.

1.3. Overview of research works on dynamics and control of carriages in automatic wood sawing lines using vertical band saws

1.3.1. Research works in the world

The dynamics and control in the sawing process of an automatic sawmill have a great influence on productivity, sawing quality and safety, especially the dynamics and control for bandsaws and wagons.

Regarding research projects on the braking system of carriages in automatic wood sawing lines, the braking system of carriages carrying wood has been developed relatively completely for automatic wood sawing systems and ensures safety in case of accidents. However, there has not been any publication in the world related to the research on the braking system of carriages carrying wood.

Regarding the vibration of carriages in automatic sawmilling lines, there has been no published research on the vibration of carriages in sawmilling lines.

1.3.2. Research works in Vietnam

Currently in Vietnam, there are a number of automatic wood sawing lines using vertical band saws and wood carts that are now relatively complete and widely applied in actual production, especially in developed countries, but the publications on the research results of wood carts in wood sawing lines in general and automatic wood sawing lines in particular in the world and in Vietnam are still very limited, especially research works on dynamics and control of wood carts. There are some publications on research on wood sawing lines in general but mainly focus on the stability of vertical band saws, the grinding between the saw blade and the flywheel and some studies related to experimental methods to optimize the longitudinal speed of the cart and studies on the performance of wood sawing lines. Studies on control, braking and lateral vibration of wood carts have almost not been published.

1.4. Overview of the structure and operating principle of the carriage in the automatic wood sawing line designed and manufactured by project code DTĐL.CN-10/16

The wood carriage system in the automatic wood sawing line is the most important system, determining the productivity and quality of the product. This is the system with the most complex structure and the most details in the line. The carriage system in the automatic wood sawing line includes the following structures:

- Log rotation mechanism to create optimal sawing position;
- The clamping mechanism tightly clamps the log to stabilize the log when sawing to prevent shaking or shifting;
- Mechanism to move the log into the saw to create the thickness of the saw grain;
- Mechanism to move the carriage along the length of the tree to create saw veins.

The system of rotating, flipping, and clamping wood in the automatic wood sawing line has been designed.

Working principle

The automatic wood sawing equipment line is designed with a capacity of 3-4 m3 of finished products/hour. The input of the line is round wood with a diameter of 0.3-0.8m, maximum length of 4m, the thickness of finished wood reaches an accuracy of ≥ 0.8mm/total length of 4m, the wood ratio reaches 60-70%. The rotating and tilting system, the wood clamp in the automatic wood sawing line is the most important system, determining the productivity and quality of the product. This is the system with the most complex structure and the most details in the line.

The wood carriage can move through 6 wheels placed on two steel rails. Although the carriage runs on the iron rails at a low speed, only about 0.08 - 0.25 m/s, but due to the large weight, unevenly distributed on the 6 wheels moving on two iron rails placed on the elastic concrete floor, it will lead to vibration of the rails with different amplitudes and frequencies; this is one of the reasons that makes the wood sawing plane vibrate horizontally, leading to an increase in the width of the sawing joint as well as the quality. The sawn surface is reduced. Therefore, it is necessary to study this content in depth to find suitable parameters in the design and initial installation of the wood carriage system, ensuring that the sawn amplitude is within the allowable limit during the sawing process. This is also one of the research purposes of the thesis.

1.5. Research objectives of the thesis

Based on the results of the overview analysis, to serve the research purpose, the thesis needs to complete the following research objectives:

- Build a model, establish dynamic equations in the longitudinal motion of the carriage on the rail, from there simulate controlling the carriage to run at a speed suitable to the parameters of the saw blade cutting force and the specific cutting resistance of the wood.
- Establish the horizontal oscillation equation of the sawn wood joint, survey the factors affecting the horizontal oscillation amplitude of the sawn wood joint, calculate the parameters of the foundation and rails to serve the initial installation process, ensure that the maximum horizontal oscillation amplitude of the sawn wood joint must be within the allowable limit.
- Calculate the parameters for the brake cable and the brake pulling force as well as the brake cable reverse pulling speed so that when the carriage is braked (braked by winch), the braking distance is within the allowable distance.

- Experiment to verify whether the theoretical calculation model of transverse oscillation of the saw blade is consistent with reality.

1.6. Research subjects

The research object in the thesis is the carriage system in the automatic wood sawing line designed and manufactured by the state-level project code DTĐL.CN-10/16.

1.7. Scope of research

- To build a theoretical model when studying the horizontal oscillation of the saw blade as well as the braking process, the thesis uses the following assumptions:

+ The frame and wheels of the cart are absolutely rigid (not subject to bending, twisting, or compression);

+ The carriage wheels roll without slipping on the rails;

+ Pure bending rails, placed on Winkler elastic foundation;

+ Brake cable has initial self-stretch and elasticity according to Huc's law;

+ Ignore the clearance between the wheels and wheel bearings as well as the clearance between the wheels and the rail beam.

- Experiments to verify the model will use Ash wood (with specific shear resistance, $K = 36.15\ N/mm^2$ [3]) for sawing experiments .

1.8. Research content

1.8.1. Theoretical research content

- Build a dynamic model, establish differential equations describing the longitudinal motion dynamics of the carriage;
- Build model, establish dynamic equation of braking process;
- Build controller, algorithm to control the longitudinal movement of the carriage and the braking process;
- Build a model, establish the horizontal oscillation equation of the carriage in the saw blade plane, based on the problem of a beam lying on an elastic foundation subjected to a concentrated load that changes and moves;
- Survey of dynamic equations and simulation of carriage control during longitudinal movement and braking process;
- Investigate the horizontal oscillation equation of the carriage in the saw plane when sawing wood.

1.8.2. Experimental research content

- Determine the load acting on the wheels;
- Determine the self-expansion coefficient λ of the cable;
- Determine the background coefficient k_0;
- Experimentally measure the horizontal oscillation amplitude of the slit circuit to verify with the theoretical calculation results.

1.9. Research methods

1.9.1. Theoretical research method

In theoretical research, the thesis applies the method of building a dynamic model of a carriage, taking into account the factors affecting the braking process; building a problem of lateral oscillation of a carriage, then examining the systems of equations using established algorithmic models.

1.9.2. Experimental research method

- In experimental research, the thesis applies the method of measuring non-electrical quantities by electricity, using modern measuring devices and software in collecting and processing experimental data;

- The application of the above research methods will be presented specifically in the following chapters when conducting research on each content.

Chapter 1 Conclusion

1. The automatic wood sawing carriage system has been designed and manufactured by the independent state-level project code DTĐL.CN-10/16. However, the project only focuses on design calculation, manufacturing and testing, and has not mentioned the research on the dynamics and control of this carriage.

2. In published research works on wood sawing chain systems in the world and in Vietnam, the research content on dynamics and control of automatic wood sawing carriages is still limited.

3. The automatic wood sawing carriage system designed and manufactured by the independent state-level project still has many shortcomings, such as large vibrations, which affect the unevenness of the sawn surface, the length of the braking distance of the carriage is large when the carriage has an accident, thereby affecting the safety of the saw blade. Therefore, the implementation of the topic: ***"Research on dynamics and control of carriages in automatic wood sawing lines"*** that the thesis chose is necessary to provide solutions to select and control reasonable parameters in the wood sawing process; limit vibrations and brake promptly when the carriage has an accident, thereby increasing sawing productivity, ensuring quality and safety for the automatic wood sawing carriage system .

CHAPTER 2 DYNAMICS AND CONTROL OF Carriages DURING MOVEMENT, BRAKE

2.1. Dynamics and control of longitudinal motion of carriage during sawing process

When working, the carriage has two directions of movement: movement in the direction of sawing wood and movement in the direction of not sawing wood.

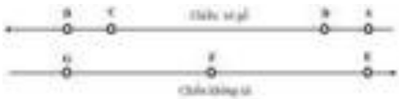

Figure 2.1 1Diagram of the movement of the carriage

The moving diagram of the carriage is shown in Figure 2.1. From this model we will analyze the forces acting on the carriage during operation.

Figure 2.2 2Dynamic model of longitudinal motion of a carriage

2.1.1. Assumptions for building a dynamic model of a carriage

- Absolutely horizontal rail;

- Ignore wind resistance because the chain is placed indoors and moves at slow speed;
- Does not take into account saw blade vibration.

2.1.2. Establish the differential equation of motion for the longitudinal motion of the carriage

From figure 2.2, we have the following force balance equation:

$$m\ddot{x} = F_k - Q_c - \Sigma F_{msi} \qquad (2.1)$$

in which: F_k - carriage cable pulling force; Q_c - resistance force of saw blade to carriage in longitudinal direction of timber; ΣF_{ms} - total friction force between carriage and rail:

$$\Sigma F_{ms} = F_1 + F_2 + F_3 + F_4 + F_5 + F_6 \qquad (2.2)$$

in which: $F_{1 \div 6}$ are the frictional forces at wheels 1 to 6 respectively.

2.2. Building a carriage motion control algorithm

To control the movement of the carriage according to the desired trajectory (running along the AB-BC-CD trajectories when sawing wood, running along the GF, FE trajectories when returning without sawing), the carriage system needs to be controlled in a closed loop, with the general control diagram shown in Figure 2.4.

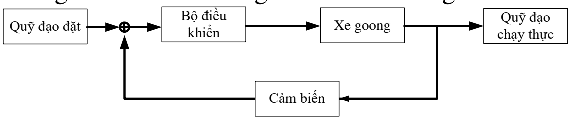

Figure 2.4 3Closed-loop control system of carriage movement

2.2.1. Setting the mode for the movement of the carriage

Setting the mode for the carriage's movement is to set the desired value of the carriage's movement to have a signal input to the control system. The design of the carriage's movement mode has the task of modeling the movement requirement (*shown in Figure 2.1*) into a mathematical signal. From the technological requirements for the carriage's movement, we can see:

When the wood-cutting cart is required to move in the 2-1-2 mode: *vehicle speed increases gradually:* section AB - *vehicle speed remains constant:* section BC - *vehicle speed decreases gradually:* section CD, this movement mode is shown above (Figure 2.5-a);

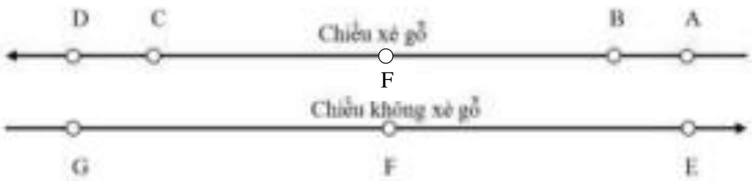

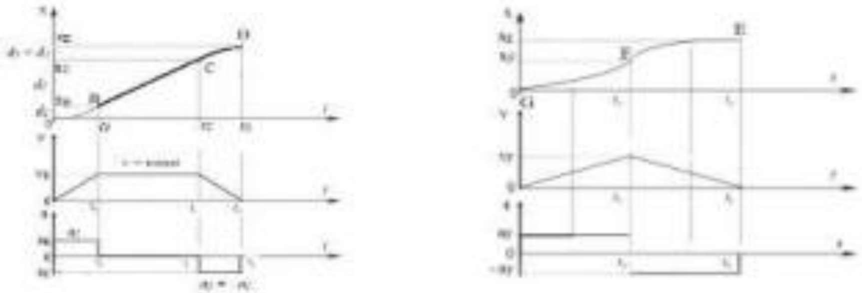

a) 2-1-2 mode b) 2-2 mode

Figure 2.5 4Graph of carriage motion mode

2.2.2. Building a carriage motion control algorithm

After the control time, $\begin{cases} e = x_d - x \to 0 \\ \dot{x} \to 0 \end{cases} \Leftrightarrow \begin{cases} x = x_d \\ \dot{x} \to 0 \end{cases}$. This means that if the friction-compensated PD controller is used, the moving *x coordinate* of the carriage will stick to the desired value; at the same time, $\dot{x} \to 0$ it means that the control system will stop the carriage at the end of the trajectory (point D for the sawing motion, and E for the return motion).

2.3. Calculation of horizontal vibration of the carriage (oscillation of the wood saw plane) during the wood cutting process

The study of the vibration of a wood carriage during the sawing process is modeled on the vibration problem of a beam on an elastic foundation (Winkler), subjected to changing and moving concentrated loads.

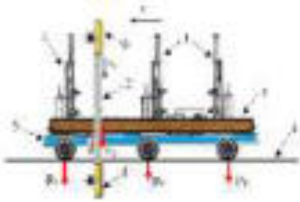

Figure 2.6 5Vertical cross-section diagram of a wood cart (in a sawing line using a vertical band saw)

In the research content of the thesis, using the Winkler elastic foundation beam oscillation model, the analytical solution of the differential equation of oscillation of the beam under mobile concentrated load is solved by the method of separation of variables. Together with the use of the Dirac Delta function and its properties, the expression for calculating the horizontal oscillation amplitude of the wood sawn joint plane is determined. Based on this result, the pair of values *EI* and k_0 is determined so that the maximum horizontal oscillation amplitude of the wood sawn joint is within the allowable limit.

2.3.1. Calculate the forces exerted by the weight of the wood carriage (in a wood sawing line using a vertical band saw) on the two rails at the contact points between the wheel

and the rail, when the carriage moves at a constant speed $v(m/s)$ ***- taking into account the wood cutting force of the saw blade***

Assuming the wooden cart frame is absolutely rigid, the axles of the 6 wheels are attached to the frame at points A_i with distances as illustrated in (Figure 2.7). At point A_i there is a shear force *Pi (N)* and at point *M there is a* downward shear force F_{c} *on the wood.*

Suppose that the wheels of the carriage, with the forces applied as above (Figure 2.7), are placed on elastic springs with stiffness coefficient $\bar{k}$. If we call F_i the force of the carriage acting on the rail beam at the points A_i (contact points of the wheels and the rail) and Wi is the length of the compressed spring (Figure 2.7), then $F_i = \bar{k}\,W_i$

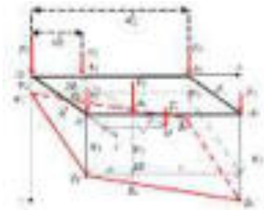

Figure 2.7 6Model for calculating the load acting on the rails at the contact points with the carriage wheels.

2.3.2. Calculation of beams on Winkler elastic foundation

2.3.2.1. Winkler's hypothesis (1867) is used to calculate beams on elastic foundations.

Beams working on elastic foundations are used with Winkler's hypothesis:

The Winkler hypothesis is a locally settled foundation, meaning that the settlement of the foundation only occurs at points below the beam, so the foundation can be described as a system of countless independent vertical springs close together (Figure 2.8a). Therefore, the reaction force intensity of the foundation at each point is proportional to the settlement of the foundation (or deflection of the beam) at that point.

According to Winkler we have: $p_0(x,t)=k_0W(x,t)$

(2.51)

in which: *W(x,t)* - Settlement of the foundation (or deflection of the beam) at the cross-section with coordinates x, *m;*

k_0 - Base coefficient, N/m^3;

$p_0(x,t)$ - Reaction of the foundation at x, N/m^2.

If the beam has a width $b<<L$ with L being the length of the beam, then it can be assumed that the reaction force of the foundation is distributed uniformly along the width b. Then, the reaction force of the foundation acting on *the cross-section* at coordinate x will be:

$$P(x,t)=k_0.b.W(x,t)=k.W(x,t),\ N/m \qquad (2.52)$$

The coefficients k_0, k are called background coefficients with dimensions

$[k_0]=\frac{N}{m^3}$, $[k]=\frac{N}{m^2}$

2.3.2.2. Dirac function

1) The Heaviside unit step function is a function of the form: $H(\xi)=\begin{cases}1\ ,\ \xi>0\\0\ ,\ \xi<0\end{cases}$ (2.53)

2) Impulse function $\delta_\varepsilon\left(x-x_0\right)=\dfrac{1}{\varepsilon}\left[H\left(x-x_0\right)-H\left(x-(x_0+\varepsilon)\right)\right]$ (2.54)

The impulse function has height $\frac{1}{\varepsilon}$ in the interval $[x_0, x_0+\varepsilon]$ and is zero elsewhere.

3) Dirac Delta Function

The Dirac Delta function is not a function in the usual sense. The Dirac Delta function is zero everywhere except at the point x_0 where it has an infinite value such that:

$$\int_{-\infty}^{+\infty}\delta(x-x_0)dx=1 \qquad (2.55)$$

2.3.2.3 Differential equation of vibration of beam on Winkler elastic foundation

Consider a beam of length *L,* with hinges at both ends, Young's modulus *E* , moment of inertia of the beam *I,* placed on a Winkler foundation with elasticity coefficient k_0. Choose the coordinate system O_{xz} with the $O_{x\ axis}$ along the beam axis, the $O_{z\ axis}$ pointing downward. The beam is subjected to a load distributed along the beam with intensity q(x,t) (N/m). Suppose that during operation the beam and the foundation are not separated, that is, the settlement of the foundation and the deflection of the beam are always equal at all cross-sections with any coordinates x.

Assuming the beam width is b , then according to Winkler there is a foundation reaction acting on the cross-section at coordinate x :

$$P(x,t)=k_0.b.W(x,t)=k.W(x,t) \qquad (2.59)$$

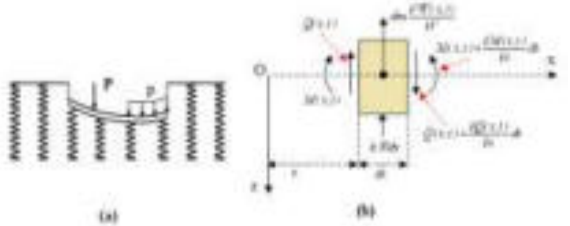

Figure 2.8 7(a) - Winkler foundation model, (b) - Description of forces acting on beam elements

$$\frac{\partial^2W(x,t)}{\partial t^2}+\frac{EI}{\rho}\frac{\partial^4W(x,t)}{\partial x^4}+\frac{k}{\rho}W(x,t)=0\ ,\ 0\le x\le L \qquad (2.67)$$

In which: *EI* (Nm^2) is the bending stiffness of the rail beam, ρ (*kg/m*) is the mass density of the rail beam per unit length.

Equation (2.67) is the *free oscillation equation* of a homogeneous beam with a constant cross-section lying on an elastic foundation with foundation coefficient $k=k_0.b$.

In the case of a beam loaded according to the distribution *q(x,t) (N/m),* we obtain the differential equation of oscillation of the beam:

$$\frac{\partial^2 W(x,t)}{\partial t^2}+\frac{EI}{\rho}\frac{\partial^4 W(x,t)}{\partial x^4}+\frac{k}{\rho}.W(x,t)=\frac{1}{\rho}q(x,t) \qquad (2.68)$$

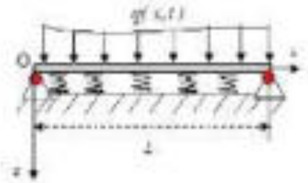

Figure 2.9 8Beam model on elastic foundation bearing distributed load *q(x,t)*

The general solution of the differential equation (2.67) is found by the method of separation of variables.

$$W(x,t)=\sum_{n=1}^{\infty}\left[A_n\cos\omega_n t+B_n\sin\omega_n t\right]\left[C_n\cos\frac{n\pi}{L}x+D_n\sin\frac{n\pi}{L}x\right] \qquad (2.69)$$

In which: A_n, B_n - are coefficients determined from initial conditions;

C_n, D_n - are coefficients determined from the boundary conditions at $x=0$ and $x=L$.

Substitute (2.69) into (2.67) to get:

$$\sum_{n=1}^{\infty}\left[-\omega_n^2+\frac{EI}{\rho}\left(\frac{n\pi}{L}\right)^4+\frac{k}{\rho}\right]\left[A_n\cos\omega_n t+B_n\sin\omega_n t\right]\left[C_n\cos\frac{n\pi}{L}x+D_n\sin\frac{n\pi}{L}x\right]=0$$

and since the expression is true for all x and t, we get: $\omega_n^2=\frac{EI}{\rho}\left(\frac{n\pi}{L}\right)^4+\frac{k}{\rho}$, $n=1,2,...$

(2.70)

2.3.2.4. Differential equation of oscillation of a beam on an elastic foundation, with two supporting ends, subjected to a load $q_0=a+bt$ moving at a constant velocity v(m/s) along the beam

Consider a beam on an elastic foundation bearing a load $q_0=a+bt$ moving at a constant velocity v (Figure 2.10)

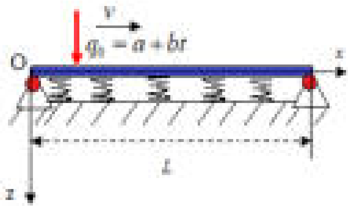

Figure 2.10 9Calculation model of elastic foundation beam vibration under load $q_0=a+bt$ moves with velocity *v*

Using the Dirac Delta function, the load distribution on the beam in this case has the form $q(x,t)=(a+bt)\delta(x-vt)$, leading to equation (2.68) having the form:

$$\frac{\partial^2 W(x,t)}{\partial t^2}+\frac{EI}{\rho}\frac{\partial^4 W(x,t)}{\partial x^4}+\frac{k}{\rho}.W(x,t)=\frac{(a+bt)}{\rho}\delta(x-vt) \qquad (2.71)$$

Find the solution (2.71) in the form: $W(x,t)=\sum_{i=1}^{\infty}T_i(t).X_i(x)$

(2.72)

Since the boundary conditions need to be satisfied: $W(0)= W(L)= 0\ ;\ \ddot{W}(0)=W(L)= 0$

(2.73)

leads to $W(x,t)=\sum_{i=1}^{\infty}T_i(t)\sin\frac{i\pi}{L}x$ (2.74)

Substituting (2.74) into (2.71) gives:

$$\sum_{i=1}^{\infty}\left[\ddot{T}_i+\left(\frac{EI}{\rho}\left(\frac{i\pi}{L}\right)^4+\frac{k}{\rho}\right)T_i\right].\sin\frac{i\pi}{L}x=\frac{(a+bt)}{\rho}\delta(x-vt) \quad (2.75)$$

Multiplying both sides of (2.75) by $sin\frac{n\pi}{L}x$ then integrating over the segment $[0,\ L]$ and paying attention to the properties of the Dirac Delta function, we get:

$$\ddot{T}_n+\left(\frac{EI}{\rho}\left(\frac{n\pi}{L}\right)^4+\frac{k}{\rho}\right)T_n=\frac{2(a+bt)}{\rho L}\int_0^L\delta(x-vt)\sin\frac{n\pi x}{L}dx=\frac{2(a+bt)}{\rho L}\sin\frac{n\pi}{L}vt \quad (2.76)$$

Equation (2.76) has the form: $\ddot{T}_n+\omega_n^2T_n=(A+Bt)\,sin\,\Omega_nt$ (2.77)

In which $\omega_n=\sqrt{\frac{EI}{\rho}\left(\frac{n\pi}{L}\right)^4+\frac{k}{\rho}}$ the natural oscillation frequency of the beam; $\Omega_n=\frac{n\pi v}{L}$ is the forced oscillation frequency and $A=\frac{2a}{\rho L}\ ;\ B=\frac{2b}{\rho L}$ (2.78)

The general solution of (2.77) will be:

$$T_n=A_n\,cos\,\omega_nt+B_n\,sin\,\omega_nt+\frac{1}{\left(\omega_n^2-\Omega_n^2\right)}\left[(A+Bt)\,sin\,\Omega_nt-\frac{2\Omega_nB}{\left(\omega_n^2-\Omega_n^2\right)}cos\,\Omega_nt\right] \quad (2.79)$$

This leads to the solution of (2.71) being:

$$W(x,t)=\sum_{n=1}^{\infty}\left\{A_n\cos\omega_nt+B_n\sin\omega_nt+(K_n+M_nt)\sin\Omega_nt+N_n\cos\Omega_nt\right\}.\sin\frac{n\pi}{L}x \quad (2.80)$$

In which: $K_n=\frac{2a}{\rho L\left(\omega_n^2-\Omega_n^2\right)};M_n=\frac{2b}{\rho L\left(\omega_n^2-\Omega_n^2\right)}\ ;N_n=-\frac{4\Omega_nb}{\rho L\left(\omega_n^2-\Omega_n^2\right)^2}$ (2.81)

2.3.2.5. Differential equation of oscillation of a beam on an elastic foundation subjected to three loads $q_1=a_1+b_1t$, $q_2=a_2+b_2t$, $q_3=a_3+b_3t$ at different positions, the loads moving at constant velocity v along the beam.

Consider a beam placed on an elastic foundation carrying three loads $q_1=a_1+b_1t$, $q_2=a_2+b_2t$, $q_3=a_3+b_3t$ the loads are spaced as shown in (Figure 2.11) and they move along the beam at a v constant speed.

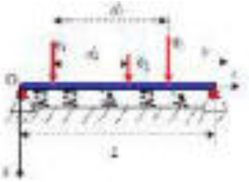

Figure 2.11 10Calculation model of beam oscillation on elastic foundation, subjected to 3 changing concentrated loads q 1, q 2 , q 3 and moving on the beam with constant velocity v .

Using the Dirac Delta function for the distributed load on the beam, the differential equation of vibration (2.71) of the beam in this case has the form:

$$\frac{\partial^2 W(x,t)}{\partial t^2}+\frac{EI}{\rho}\frac{\partial^4 W(x,t)}{\partial x^4}+\frac{k}{\rho}W(x,t)= \tag{2.82}$$
$$=\frac{1}{\rho}\left[q_1\delta(x-vt)+q_2\delta(x+d_1-vt)+q_3\delta(x+d_2-vt)\right]$$

To satisfy the boundary condition (2.73), we find the solution (2.82) in the form:

$$W(x,t)=\sum_{n=1}^{\infty}T_n(t)\sin\frac{n\pi}{L}x \tag{2.83}$$

Then T_n will be the solution of the equation:

$$\ddot{T}_n+\omega_n^2T_n=\frac{2}{\rho L}\left[q_1\sin\frac{n\pi}{L}vt+q_2\sin\frac{n\pi}{L}(vt-d_1)+q_3\sin\frac{n\pi}{L}(vt-d_2)\right] \tag{2.84}$$

Equation (2.84) becomes: $\ddot{T}_n+\omega_n^2T_n=\sum_{i=1}^{3}\left(\bar{a}_i+\bar{b}_i t\right)sin\left(\Omega_n t-\bar{c}_i\right)$ (2.87)

The general solution of (2.87) has the following form:

$$T_n(t)=A_n\cos\omega_n t+B_n\sin\omega_n t+ \tag{2.88}$$
$$+\frac{1}{\left(\omega_n^2-\Omega_n^2\right)}\sum_{i=1}^{3}\left[\left(\bar{a}_i+\bar{b}_i t\right)\sin\left(\Omega_n\,\mathrm{t}-\bar{\mathrm{c}}_i\right)-\frac{2\Omega_n\bar{b}_i}{\left(\omega_n^2-\Omega_n^2\right)}\cos\left(\Omega_n\,\mathrm{t}-\bar{\mathrm{c}}_i\right)\right]$$

leads to the general solution of (2.82) of the form:

$$W(x,t)=\sum_{n=1}^{\infty}\left\{A_n\cos\omega_n t+B_n\sin\omega_n t+\frac{1}{\left(\omega_n^2-\Omega_n^2\right)}\sum_{i=1}^{3}\left[\left(\bar{a}_i+\bar{b}_i t\right)\sin\left(\Omega_n\,\mathrm{t}-\bar{\mathrm{c}}_i\right)-\right.\right. \tag{2.89}$$
$$\left.\left.-\frac{2\Omega_n\bar{b}_i}{\left(\omega_n^2-\Omega_n^2\right)}\cos\left(\Omega_n\,\mathrm{t}-\bar{\mathrm{c}}_i\right)\right]\right\}\sin\frac{n\pi}{L}x$$

Let (2.89) satisfy the initial condition $W\big|_{t=0}=0\ ;\ \frac{\partial W}{\partial t}\Big|_{t=0}$, we get:

$$A_n = \frac{1}{\left(\omega_n^2 - \Omega_n^2\right)} \sum_{i=1}^{3} \left[\bar{a}_i \, sin\bar{c}_i + \frac{2\Omega_n \bar{b}_i}{\left(\omega_n^2 - \Omega_n^2\right)} cos\bar{c}_i \right] \tag{2.90}$$

$$B_n = \frac{1}{\omega_n \left(\omega_n^2 - \Omega_n^2\right)} \sum_{i=1}^{3} \left[\bar{b}_i \, sin\bar{c}_i - \bar{a}_i \Omega_n \, cos\bar{c}_i + \frac{2\Omega_n \bar{b}_i}{\left(\omega_n^2 - \Omega_n^2\right)} sin\bar{c}_i \right]$$

2.3.3. Equation of horizontal oscillation of the carriage (oscillation of the wood sawing plane) during the wood cutting process

2.3.3.1. Horizontal oscillation amplitude of the saw blade at a point with height h relative to the plane of the two rails

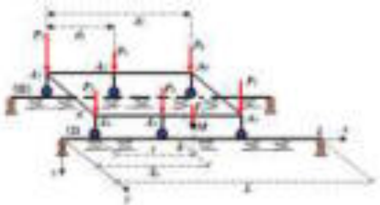

Figure 2.12 11Model of vibration of the carriage during the wood cutting process

A wood carriage (in a sawmill line using a vertical band saw) is arranged to run on two rails of the same width *b (m) and they are spaced d (m)* apart ; the loads Pi at points $A_i \, (i = 1 \div 6)$ on the wheel axles are spaced as (Figure 2.12). The rails have length *L (* m) and constant bending stiffness *EI* . The rails are placed on a concrete foundation with elasticity coefficient $k_0 \, (N/m^3)$.

Choose a coordinate system with the **x- axis** - in the direction of the rail and the **z- axis** - downward. The saw blade position is at M, with coordinates $(X_c, u, -h)$ (height h compared to the plane of the two rails). The wooden cart moves at a constant velocity v (m/s). According to the calculation in part (2.1.1), the forces acting on the rails at the points of contact with the wheels have the form: $F_i = a_i + b_i.t$

Let φ be the rotation angle around the axis x of the wood slot plane, resulting in:

$$\tan\varphi = \frac{W^{(I)}(X_c, t) - W^{(II)}(X_c, t)}{d} \tag{2.95}$$

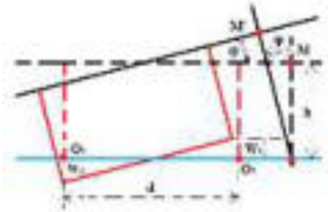

Figure 2.13 12Model for calculating angle φ – rotation angle around the Ox axis of the horizontal plane

If the oscillation is small there will be $tan\,\varphi \approx \varphi$, So:

$$\varphi(t)=\frac{1}{d}\sum_{n=1}^{\infty}\sin\frac{n\pi}{L}X_c\left\{\left(A_n^{(1)}-A_n^{(2)}\right)\cos\omega_n t+\left(B_n^{(1)}-B_n^{(2)}\right)\sin\omega_n t+\right. \quad (2.96)$$

$$\left.+\frac{1}{\left(\omega_n^2-\Omega_n^2\right)}\sum_{i=1}^{3}\left[\left(\bar{a}_i^{(1)}-\bar{a}_i^{(2)}+\left(\bar{b}_i^{(1)}-\bar{b}_i^{(2)}\right)t\right)\sin\left(\Omega_n\,\mathrm{t}-\bar{c}_i\right)-\frac{2\Omega_n\left(\bar{b}_i^{(1)}-\bar{b}_i^{(2)}\right)}{\left(\omega_n^2-\Omega_n^2\right)}\cos\left(\Omega_n\,\mathrm{t}-\bar{c}_i\right)\right]\right\}$$

The horizontal oscillation amplitude of the saw blade at point - with height h above the rail surface will be:

$$A=h.\varphi(t) \quad (2.97)$$

In expression (2.96), the right-hand side is a function series. If $\Omega_n\neq\omega_n$ (when no resonance occurs), then the coefficients are infinitesimally small on the order of $\frac{1}{n^2}$ when $n\rightarrow\infty$, so the series converges uniformly for all x and t. Therefore, when calculating, we will take the sum of a finite number of terms and can evaluate this error.

2.3.4. Resonance test

Equation (2.97) - represents the amplitude of horizontal oscillation of the saw plane at a point of height h - resonance phenomenon (or beat phenomenon) will occur if the natural oscillation frequency ω_n coincides (or is close to) the forced oscillation frequency Ω_n. From the expression in (2.94), in order for $\omega_n=\Omega_n$ (i.e. when the resonance phenomenon will occur) the velocity v must be satisfied:

$$v^2=\frac{\left[\frac{EI}{\rho}\left(\frac{n\pi}{L}\right)^4+\frac{k}{\rho}\right]}{\left(\frac{n\pi}{L}\right)^2} \quad (2.98)$$

Thus, the beat phenomenon will occur if the velocity of the carriage is in the vicinity of the values indicated in (2.98).

Calculating with parameters $EI=30\times10^6\,Nm^2$; $\rho=40\ kg/m$; $L=15\ m$; $k=6\times10^6\ N/m^2$, from (2.98) we will get the values of *v (m/s)* corresponding to the mod *n* for resonance to occur, the calculation results are recorded in (Table 2.1).

.

Table 2.1 1The speed v of the carriage for resonance to occur corresponds to the mod n

mod (n)	$\omega_n=\Omega_n$ (Hz)	$v(m/s)$	mod (n)	$\omega_n=\Omega_n$ (Hz)	$v(m/s)$
1	389.2	1858.1	6	1421.4	1131.1
2	416.0	993.2	7	1901.3	1296.9
3	516.6	822.2	8	2461.9	1469.3
4	720.7	860.3	9	3101.3	1645.3
5	1025.6	979.4	10	3818.5	1823.2

According to the results obtained in Table 2.1, it can be seen that the resonance phenomenon occurs at the smallest velocity of 822.2 (m/s) (with mod n=3). Therefore, with the velocity of the carriage only in the range of 0.09 - 0.25 (m/s), resonance cannot occur.

2.4. Carriage brake mechanism and dynamic calculation model when braking

2.4.1. Vehicle brake mechanism

Because the carriage has a large mass and runs on rails, even though it moves at a low speed, if a brake system is used to clamp the wheels, the carriage will still slide on the rails when braking. Therefore, here the carriage brake will be used with a cable pulling back when braking.

The carriage brake mechanism consists of a steel cable connecting the carriage to the cable pulling system located at A - firmly attached to the ground as shown (Figure 2.14).

Steel cables are braided with steel strands, each steel strand is braided with steel fibers. Note that, because they are braided with fibers, when pulling the cable, there will be self-stretching (until the fibers and strands make the cable tight), at that time the cable pulling force will have an impact on the brake. The self-stretching of the cable is evaluated through the coefficient λ , that is, if the cable has an initial length $L_0 (m)$, after self-stretching it has a length $L_d (m)$, then we get:

$$\lambda = \frac{L_d - L_0}{L_0} \qquad (2.99)$$

The brake cable pulling system is required to start and work in a very short time (<< 1s), so it should be designed with a hydraulic system. The brake cable pulling system creates a cable pulling force so that the brake cable moves with an acceleration a_k .

2.4.2. Calculation model of vehicle braking dynamics

Suppose during the process of sawing wood, the car moves in direction AB, when it reaches B, the car brakes.

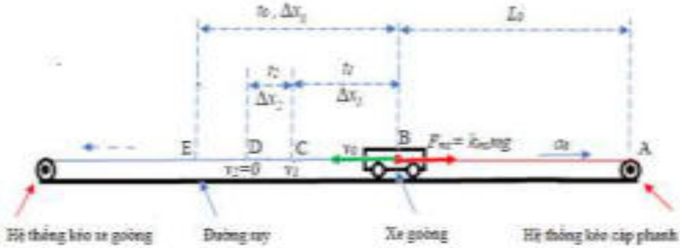

Figure 2.14 13Dynamic calculation model when braking a carriage

In fact, when starting to brake, the brake cable moves in the direction BA with acceleration a_k . Because at the initial moment the brake cable has a velocity of 0, after time t_0 , the brake cable is rolled onto roller A with a length of: $L_{cuon} = \frac{a_k t_0^2}{2}$

(2,107)

With initial length L_0 , the cable has self-stretching length: $L_{dan} = \lambda . L_0$

(2.108)

During braking, the following situations may occur:

If $\Delta x_0 \leq L_{dan} - L_{cuon} = \lambda L_0 - \frac{a_k t_0^2}{2} \iff v_0^2 \leq \frac{2 g^2 . k_{ms}^2 \lambda L_0}{\left(g k_{ms} + a_k \right)}$ (2.109) then no brake needed (brake not working)

If $\Delta x_0 > L_{dan} - L_{cuon} = \lambda L_0 - \dfrac{a_k t_0^2}{2} \Leftrightarrow v_0^2 > \dfrac{2g^2.k_{ms}^2 \lambda L_0}{\left(gk_{ms} + a_k\right)}$ (2,110)

then the brake will work.

2.4.3. Establish the dynamic equation of the carriage during braking

As analyzed in the model of calculating the dynamics of the carriage during the movement and braking process in the above section, let v_0 be the velocity of the carriage at the beginning of braking, then there are two cases that occur:

+) The car will stop before the brakes take effect if: $v_0^2 \leq \dfrac{2g^2.k_{ms}^2 \lambda L_0}{\left(gk_{ms} + a_k\right)}$ (2.111)

+) The braking process is effective if: $v_0^2 > \dfrac{2g^2.k_{ms}^2 \lambda L_0}{\left(gk_{ms} + a_k\right)}$ (2.112)

Construct the dynamic equation for the vehicle in *the process of satisfying condition (2.112)*. Then the vehicle drifts to the time t_1 (with $t_1 < t_0$) when the vehicle brakes start to take effect. The value that t_1 satisfies the equation:

$$\Delta x_1 = -k_{ms} g.\frac{t_1^2}{2} + v_0 t_1 = \lambda L_0 - \frac{a_k t_1^2}{2} \qquad (2,113)$$

or: $$-\frac{\left(k_{ms} g - a_k\right)}{2} t_1^2 + v_0 t_1 - \lambda L_0 = 0 \qquad (2.114)$$

We have the total distance the cart travels from the time it starts braking until it stops:

$$\Delta x = \Delta x_1 + \Delta x_2 \qquad (2,140)$$

And the force required to pull the brake: $F_{ph} = \sigma.S = E\varepsilon.S = E.S.\dfrac{\Delta x_2}{L_1}$ (2.141)

2.5. Building a motion controller with the addition of a brake component

In section 2.2, the thesis has built a motion controller for the carriage, however, because the system has very large inertia, the PD controller to compensate for friction will cause calculation errors when stopping (at point D). At the same time, this controller will not work when the system has a problem and needs to stop urgently (in case of broken saw blade, case of deviated saw circuit ...).

To overcome this problem, the thesis proposes to add a brake component to the controller. The motion controller diagram when adding a brake component is shown in Figure 2.15.

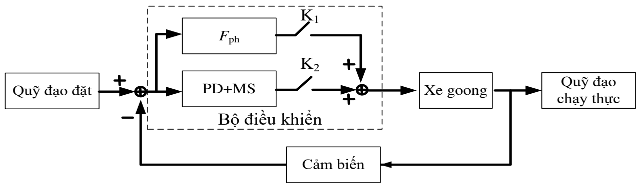

Figure 2.15. Motion controller with added brake component

Above (Figure 2.15) shows the motion controller with the addition of the brake component. The controller structure includes the PD control component compensating the friction component with equation represented in (2.37) and the brake supplement component with equation represented in (2.141). The two dynamic locks K $_1$ and K $_2$ are opened and closed in the following cases:

- In normal case $K_1 = 0$ (open), $K_2 = 1$ (closed). Then the controller equation is:

$$F_k = K_p e - K_d \dot{x} + mg\mu \tag{2.142}$$

Chapter 2 Conclusion

1. Built a model, established equations and algorithms to control the movement of the carriage during the automatic wood cutting process.
2. The horizontal oscillation model of the wood sawn joint plane has been built, the horizontal oscillation equation of the sawn joint has been established and the solution has been found in analytical form. The results obtained expressions for the natural oscillation frequency and forced oscillation allow checking the resonance of the oscillation of the rail beam, this research result is the basis for investigating the horizontal oscillation of the sawn joint to determine the construction parameters, installation of the carriage track foundation
3. The model has been built and the dynamic equation of the carriage braking process has been established when the carriage encounters an accident. The motion control algorithm has been built when adding a braking component. This result is the basis for investigating the braking dynamics to propose a safe carriage braking system when in use.

CHAPTER 3 SURVEY OF DYNAMIC EQUATIONS AND TRAIN CONTROL SIMULATION DURING MOVEMENT, BRAKE

The simulation results will provide parameters to control the carriage to move at speeds appropriate to each type of wood and the size of the sawn log, ensuring proper sawing techniques and achieving the highest productivity.

3.1. Investigation of the horizontal oscillation equation of the saw circuit

Equation representing the horizontal oscillation of the sawn wood circuit (2.96)

$$\varphi(t) = \frac{1}{d}\sum_{n=1}^{\infty}\sin\frac{n\pi}{L}X_c\left\{\left(A_n^{(1)} - A_n^{(2)}\right)\cos\omega_n t + \left(B_n^{(1)} - B_n^{(2)}\right)\sin\omega_n t + \right.$$

$$\left. + \frac{1}{\left(\omega_n^2 - \Omega_n^2\right)}\sum_{i=1}^{3}\left[\left(\bar{a}_i^{(1)} - \bar{a}_i^{(2)} + \left(\bar{b}_i^{(1)} - \bar{b}_i^{(2)}\right)t\right)\sin\left(\Omega_n t - \bar{c}_i\right) - \frac{2\Omega_n\left(\bar{b}_i^{(1)} - \bar{b}_i^{(2)}\right)}{\left(\omega_n^2 - \Omega_n^2\right)}\cos\left(\Omega_n t - \bar{c}_i\right)\right]\right\}$$

In there: $\bar{c}_1 = 0\ ;\ \bar{c}_2 = \frac{n\pi}{L}d_1\ ;\ \bar{c}_3 = \frac{n\pi}{L}d_2$

$$\bar{a}_1^{(1)} = \frac{2a_1}{\rho L};\ \bar{b}_1^{(1)} = \frac{2b_1}{\rho L};\ \bar{a}_2^{(1)} = \frac{2a_4}{\rho L};\ \bar{b}_2^{(1)} = \frac{2b_4}{\rho L};\ \bar{a}_3^{(1)} = \frac{2a_5}{\rho L};\ \bar{b}_3^{(1)} = \frac{2b_5}{\rho L};$$

$$\overline{a}_1^{(2)} = \frac{2a_2}{\rho L};\ \overline{b}_1^{(2)} = \frac{2b_2}{\rho L};\ \overline{a}_2^{(2)} = \frac{2a_3}{\rho L};\ \overline{b}_2^{(2)} = \frac{2b_3}{\rho L};\ \overline{a}_3^{(2)} = \frac{2a_6}{\rho L};\ \overline{b}_3^{(2)} = \frac{2b_6}{\rho L};$$

$$A_n^{(m)} = \frac{1}{\left(\omega_n^2 - \Omega_n^2\right)} \sum_{i=1}^{3} \left[\overline{a}_i^{(m)} \sin\overline{c}_i + \frac{2\Omega_n \overline{b}_i^{(m)}}{\left(\omega_n^2 - \Omega_n^2\right)} \cos\overline{c}_i \right]$$

$$B_n^{(m)} = \frac{1}{\omega_n \left(\omega_n^2 - \Omega_n^2\right)} \sum_{i=1}^{3} \left[\overline{b}_i^{(m)} \sin\overline{c}_i - \overline{a}_i^{(m)} \Omega_n \cos\overline{c}_i + \frac{2\Omega_n \overline{b}_i^{(m)}}{\left(\omega_n^2 - \Omega_n^2\right)} \sin\overline{c}_i \right]; \quad m = 1,\ 2$$

$$\omega_n^2 = \frac{EI}{\rho}\left(\frac{n\pi}{L}\right)^4 + \frac{k}{\rho};\ \Omega_n = \frac{n\pi v}{L}$$

The amplitude of horizontal oscillation A is calculated according to A = h.φ(t)

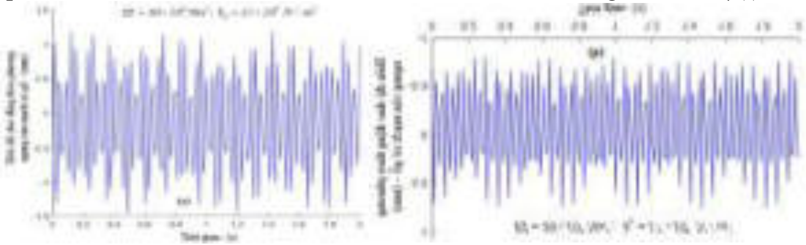

Figure 3.1 1Horizontal vibration amplitude of wood cutting circuit

Calculate with the parameters in Table 3.1 and the loads placed at the points A_i:

$P_1 = 10kN;\ P_2 = 9kN; P_3 = 8{,}5\ kN; P_4 = 9{,}2kN; P_5 = 10{,}5\ kN; P_6 = 10{,}2\ kN;$

The number of terms taken from the total *N=30* . The calculation results of the horizontal oscillation amplitude at *M* located on the saw blade plane with height *h=1.2* (m) are shown in (Figure 3.1) with two cases: $EI = 30\times10^6\ Nm^2;\ k = 12\times10^5\ N/m^2$ and $EI = 80\times10^6\ Nm^2;\ \ k = 17\times10^5 N/m^2$.

The calculation results in a period of *120 s* (time to cut a *6 m long log*) show that the horizontal oscillation amplitude at the point on the saw plane (*1.2 m high*) reaches the maximum value of *1.5 mm* in case (a) and *0.82 mm* in case (b) (Figure 3.1)

Comment:

From the survey results for two cases when increasing the value of *EI* as well as increasing the value of k, the maximum horizontal oscillation amplitude will also decrease. To be able to evaluate the reduction level of the horizontal oscillation amplitude of the saw blade when increasing the values of *EI* and k_0, the next section will calculate the maximum horizontal oscillation amplitude corresponding to the pairs of values *EI* and k_0 change .

3.2. Investigation of the influence of parameters EI and k_0 on the maximum value of the amplitude of horizontal oscillation of the saw blade

3.2.1 Investigation of the dependence of the maximum value of the horizontal oscillation amplitude of the slit circuit on the parameters EI and k_0

In wood sawing technique, the horizontal oscillation amplitude of the sawing plane is only allowed within a very small limit (< *1.5 mm*). Therefore, in the design and construction of the wood sawing line, it is necessary to choose appropriate parameters to ensure technical requirements during the sawing process. Note that, from formulas (2.93) - (2.97), when the parameters of the carriage are fixed, the horizontal oscillation amplitude of the sawing plane depends on the parameters *EI* - the bending stiffness of the rail and k_0 - the elastic stiffness of the foundation.

For each pair of values *EI* and k_0, the maximum value of the horizontal vibration amplitude of the sawn surface will be obtained. These results are recorded in (Table 3.2) with a graph (Figure 3.2) showing the relationship between the maximum horizontal vibration amplitude A and the bending stiffness of the rail *EI* and the foundation coefficient k_0. From here, it is possible to choose pairs of values EI and k_0 so that the horizontal vibration amplitude of the sawn surface is within the allowable limit during the sawing process.

Table 3.2 1Maximum value of oscillation amplitude A(mm) in the horizontal direction of the saw plane for each pair of values EI and $k = k_0.b$.

Calculate according to the parameters in Table 3.1 and with $v = 0.15$ *m/s*; $b_0 = 0.1$ *m*

$EI.10^{-6}$ (Nm^2)	$k.10^{-5}(N/m^2)$						
	12	**13**	**14**	**15**	**16**	**17**	**18**
30	1,501	1,428	1,335	1,237	1,194	1,146	1,081
35	1,449	1.37	1,286	1,213	1,152	1,086	1,046
40	1,414	1.31	1,252	1,182	1,126	1,076	1,023
45	1,358	1,292	1,225	1,152	1.09	1,043	1,001
50	1,339	1,248	1,208	1,136	1,084	1,022	0.972
55	1,298	1.25	1,161	1,105	1.06	***0.999***	***0.956***
60	1,284	1.2	1,131	1,075	1,036	***0.983***	***0.939***
65	1,247	1.18	1,111	1,063	1,004	***0.963***	***0.925***
70	1,226	1,155	1,094	1,038	***0.994***	***0.939***	***0.905***
75	1,212	1,129	1,079	1,015	***0.98***	***0.925***	***0.9***
80	1,183	1,127	1,066	***0.994***	***0.948***	***0.92***	***0.888***
85	1,175	1,109	1,052	***0.991***	***0.945***	***0.908***	***0.839***

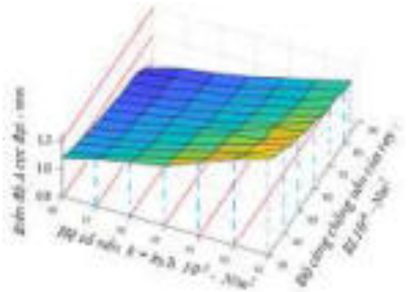

Figure 3.2 2Graph of the relationship between the maximum horizontal vibration amplitude A(mm) and the bending stiffness of the rail *EI* (Nm^2) and the stiffness coefficient of the foundation $k=k_0 b$ (N/m^2)

3.2.2 Determine the depth h of the concrete foundation for installing the carriage

When designing and installing the foundation and rail beam system for carriages, from the choice of the bending stiffness of the rail beam *EI* , using (Table 3.2), we can determine the concrete foundation coefficient that needs to be at least k_0 so that the maximum horizontal oscillation amplitude of the split joint does not exceed 1 mm.

When knowing the length *L* , width *R* of the concrete block of the foundation and the coefficient of the ground under the concrete layer is k_d , we need to determine the depth h of the concrete foundation layer so that the overall foundation coefficient reaches $k \geq k_0$.

When placing a uniformly distributed load with intensity q^* (N/m ^{2}) on the surface of the concrete foundation. Let the deflection at the midpoint O on the concrete foundation be y_O , then the foundation coefficient at O will be:

$$\lambda_O = \frac{q^*}{y_O}. \qquad (3.1)$$

According to the Winkler foundation model, the foundation reaction r(x) at each point is proportional to the elastic settlement at that point, that is, r(x) = k_d .Ry(x). The foundation reaction r(x) can be considered as a continuous, non-uniform and upward load, so we get the differential equation for the deflection of the bent beam:

$$E_b I_b \frac{d^4 y(x)}{dx^4} + k_d R.y(x) = q \qquad (3.2)$$

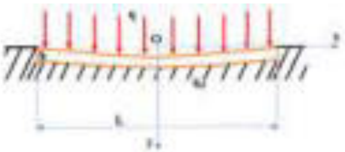

Figure 3.3 3Model of a beam bearing uniformly distributed loads on an elastic foundation

Thus, if choosing a rail beam with steel material and cross-sectional shape to achieve bending stiffness of EI = 75.10 ^{6} Nm ^{2} , requiring the joint to have the largest horizontal oscillation amplitude of 1 mm, then the foundation (soil, concrete) must have a foundation coefficient of at least $k \geq k_0$ = 16.10 ^{6} N/m ^{3} . With the concrete foundation size with length L=16 m, width R=2.2 m, the following results will be obtained:

a) With M300 concrete according to TCVN 5574:2018 with elastic modulus E_b = 28.75 MPa, the ratio $\frac{k}{k_0}$ corresponding to the ground coefficients k_d under the concrete layer (medium dense sandy soil according to Bowles) is shown in the graph (Figure 3.4). From the above graph (Figure 3.4), it can be seen that: if the ground coefficient increases, the thickness of the concrete layer will decrease. For example, $\frac{k}{k_0} = 1$ with k_d = 8 kN/m ^{3} , the M300 concrete layer needs a filling depth of h_n = 0.88 m; and with k_d = 14 kN/m ^{3} , the M300 concrete layer needs a filling depth of h_n = 0.7 m.

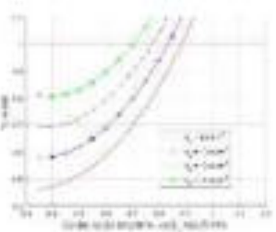

Figure 3.4 4Ratio $\frac{k}{k_0}$ according to the filling of M300 concrete layer corresponding to soil layers with foundation coefficients k $_d$

b) With the subsoil layer having a foundation coefficient k $_d$ = 10 kN/m ^{3}, the ratio $\frac{k}{k_0}$ corresponding to concrete layers with different grades (according to TCVN 5574:2018) is shown in the graph in Figure 3.5. From the graph above (Figure 3.5), it can be seen that: if the concrete grade increases, the thickness of the concrete layer will decrease. For example, for $\frac{k}{k_0} = 1$ a M200 concrete layer, the filling depth h $_n$ = 0.88 m is required; and for an M400 concrete layer, the filling depth h $_n$ = 0.8 m is required.

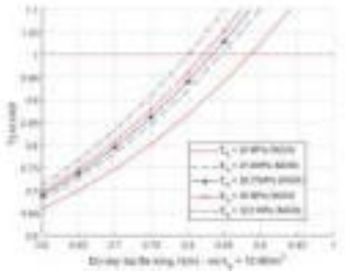

Figure 3.5 5Ratio $\frac{k}{k_0}$ according to concrete layer filling with different Mac (when the underlying soil layer has a foundation coefficient k $_d$ = 10 kN/m ^{3})

3.3. Investigation of the influence of the speed of the wood carriage on the maximum value of the amplitude of horizontal oscillation of the sawn joint

The calculation results of the maximum amplitude of horizontal vibration of the wood sawing circuit and the wood cutting force according to the moving velocity of the wood carriage are recorded in (Table 3.3) and the graph showing these dependencies is recorded in (Figure 3.6).

From this calculation result, it can be seen that when the velocity is between 0.01 m/s and 0.07, the maximum horizontal oscillation amplitude of the saw blade will increase with the same velocity. When the carriage velocity is between 0.07 m/s and 0.2 m/s, the maximum horizontal oscillation amplitude of the saw blade does not change much when the carriage velocity changes, they are almost at the same level.

Table 3. 2Maximum horizontal oscillation amplitude of sawn wood according to the values of wood carriage speed at pairs of values *(EI,k=k $_0$ b)*

EI.10 $^{-6}$ (Nm ^{2}) =	**80**	**60**	**40**
k.10 $^{-5}$ (N/m ^{2}) =	**17**	**15**	**13**
v(m/s)	*Max Amplitude (mm)*	*Max Amplitude (mm)*	*Max Amplitude (mm)*
0.03	0.86	1.01	1.23
0.04	0.90	1.05	1.27
0.05	0.92	1.08	1.31
0.06	0.94	1.09	1.34
0.07	**0.94**	**1.10**	**1.35**
0.08	0.94	1.11	1.36
0.09	0.93	1.11	1.36
0.1	0.93	1.10	1.36
0.11	0.93	1.10	1.36
0.12	0.93	1.11	1.37
0.13	0.93	1.11	1.36
0.14	0.93	1.11	1.36
0.15	0.94	1.11	1.36
0.16	0.94	1.11	1.36
0.17	0.94	1.11	1.36
0.18	0.94	1.11	1.36
0.19	0.94	1.11	1.35
0.2	0.94	1.11	1.35

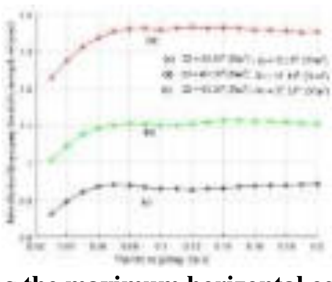

Figure 3.6 . Graph showing the maximum horizontal oscillation amplitude of the saw blade at different velocities at pairs of values of *EI* and *k* $_0$.

Comment: The maximum horizontal oscillation amplitude of the saw blade will increase nearly linearly with the velocity when the carriage velocity is in the range v = 0.03 – 0.07 m/s and will remain almost unchanged when the carriage velocity is in the range v = 0.07 – 0.2 m/s.

3.4. Survey, evaluation of dynamics and control of carriage motion through simulation

3.4.1. Carriage operating assumptions used for simulation

According to technological requirements, parameters of the carriage model:

$F_k = m\ddot{x} + B_0\dot{x} + mg\mu$ (3.10)

with $B_0 = \frac{850.Kb_c L_{cat}}{v_c}$ and parameters defined in Table 3.4

From the above assumptions, calculate the *x coordinate values* of the cart when moving in the direction of sawing wood (*equation (2.30)*) and when moving back to no load (*equation (2.34)*)

Table 3.4 3Wagon model parameters and motion requirements

STT	Parameters	Unit	Value	Note
1	L_{cat}	*m*	0.5	*Height of the slit*
2	K	N/mm^2	36.15	Specific shear resistance
3	b_c	*mm*	2.5	Width of sawn wood
4	v	*m/s*	0.15	*Wagon speed (also the speed of pushing the log)*
5	m_{xg}	*kg*	6000	
6	m_g	*kg*	500	
7	µ		0.01	Coefficient of motion drag, $\mu = \frac{k_{ms}d_b + k_t d_t}{d_b} k_b$
8	L_2	*m*	4	*Length of sawn log*
9	$L_1 = L_3$	*m*	0.5	*Distance between segment AB and CD – unsplit segment*
10	a_{max}	m/s^2	0.04	*Limit acceleration of carriage motion*

3.4.1.1. Calculate parameters in the vehicle moving mode in the direction of sawing wood

Calculate with the parameters in Tables (3.1) and (3.4), and with:

$$L_2 = 4\ (m);\ v = 0{,}15(m/s);\ L_1 = 0{,}5(m) \quad (3.11)$$

a) Call a_1 and t_B is the acceleration and time of the vehicle's motion on section AB, according to (2.30) we get the equation of motion of the vehicle on section AB:

$$x = \frac{a_1}{2}t^2\ ;\ 0 \le t \le t_B \quad (3.12)$$

according to (2.26) we get: $t_B = \frac{2L_1}{v}\ ;\ a_1 = \frac{v^2}{2L_1}$ (3.13)

Substitute (3.11) into (3.13) to get:

$$t_B = \frac{20}{3} \approx 6{,}67\ (s)\ ;\ a_1 = 0{,}225\left(\frac{m}{s^2}\right) \quad (3.14)$$

Satisfy the condition: $a_{max} = 0{,}04 > \frac{v^2}{2L_1} = 0{,}0225$ (3.15)

Because on the AB section, there is no resistance to cut the wood, so from (2.35), the traction force of the car F_{k_AB} need to satisfy the equation:

$$F_{k\_AB} = ma_1 + mg\mu \tag{3.16}$$

b) On section BC, because the car moves at a constant speed v and there is a resistance to cutting the wood, we have the equation of motion:

$$x = L_1 + v.(t - t_B) \ ; \ t_B \le t \le t_C = t_B + \frac{L_2}{v} \tag{3.17}$$

and the traction force F_{k_BC} must satisfy the equation: $F_{k\_BC} = B_0 v + mg\mu$ (3.18)

with $m = (m_{xg} + m_g)\,;(kg)$

$$B_0 = \frac{850.Kb_c L_{cat}}{v_c};\left(\frac{N.s}{m}\right)$$

$$v_c = \frac{\pi D\omega_c}{60};(m/s) \quad , \tag{3.19}$$

c) On segment CD, because the car moves gradually decreasing with acceleration $-a_1$ and there is no resistance to cutting the wood, we get the equation of motion:

$$x = L_1 + L_2 + v(t - t_c) - \frac{a_1}{2}(t - t_c)^2 \ , \ t_C \le t \le t_D = t_C + t_B \tag{3.20}$$

and the traction force F_{k_CD} must satisfy the equation:

3.4.1.2. Calculate parameters in the mode of the vehicle moving backwards and not cutting wood

The equation of motion of the cart in reverse mode without cutting wood according to (2.34) has the form:

$$x = H_1\left(t - \frac{t_{DA}}{2}\right)t - H_2\left(t - \frac{t_{DA}}{2}\right)^3 - \frac{L}{4}; \qquad 0 \le t \le t_{DA} = \sqrt{\frac{6L}{a_{max}}} \tag{3.22}$$

In there $H_1 = \sqrt{\frac{3La_{max}}{8}} \ ; \ H_2 = \frac{a_{max}}{6}\sqrt{\frac{2a_{max}}{3L}} \ ; \ t_{DA} = \sqrt{\frac{6L}{a_{max}}}$

Where a_{max} is the limiting acceleration of the carriage's motion.

Leads to:

$$\dot{x} = H_1\left(t - \frac{t_{DA}}{2}\right) - \frac{H_2}{3}\left(t - \frac{t_{DA}}{2}\right)^2; \qquad 0 \le t \le t_{DA} = \sqrt{\frac{6L}{a_{max}}} \tag{3.23}$$

Equations (3.22) and (3.23) satisfy the condition:

$$\begin{cases} x(0) = 0 \ ; \ x(t_{DA}) = L \\ \dot{x}(0) = 0 \ ; \ x(t_{DA}) = 0 \end{cases} \tag{3.24}$$

The carriage traction force F_{k_DA} must satisfy the equation:

$$F_{k\_DA} = \frac{mH_2}{6}\left(\frac{t_{DA}}{2} - t\right) + mg\mu \ ; 0 \le t \le t_{DA} = \sqrt{\frac{6L}{a_{max}}} \tag{3.25}$$

3.4.2. Simulation results

Use Matlab-Simulink software to set up the simulation program, with the system block diagram described in Figure 3.7.

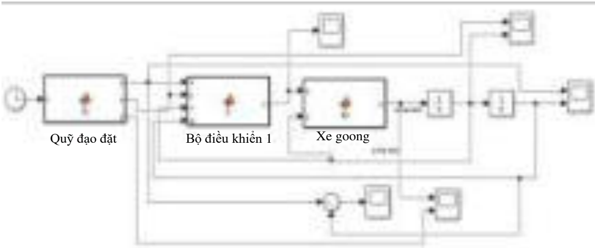

Figure 3.7. Block diagram of Matlab-Simulink being built

Q is the input trajectory block according to (3.20) or (3.22); F is controller 1 with control law in (2.37); M is the carriage model described by the dynamic equation.

3.4.2.1. Simulation with the case of moving sawmill when sawing wood

The simulation results of the process of the cart moving forward to cut wood are shown in (Figure 3.9, Figure 3.10, Figure 3.11, Figure 3.12). On (Figure 3.8) shows the variation of the *x coordinate* of the cart over time;

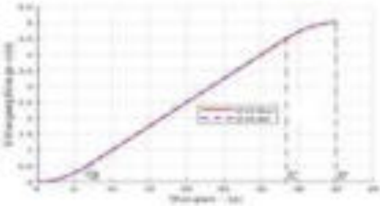

Figure 3.8. Carriage travel mode

(Shows the position of the sawn log placed on the wagon as it passes over the saw blade)

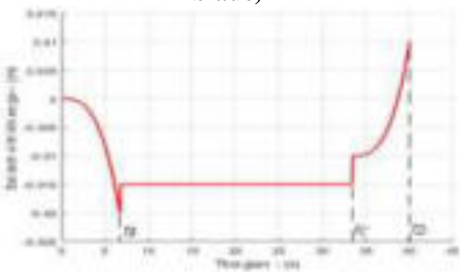

Figure 3.9. Positional deviation when the carriage moves during the sawing process (deviation = desired value - actual position)

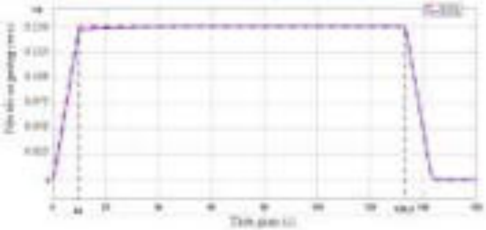

Figure 3.10. The moving speed of the cart when moving forward during the wood cutting process

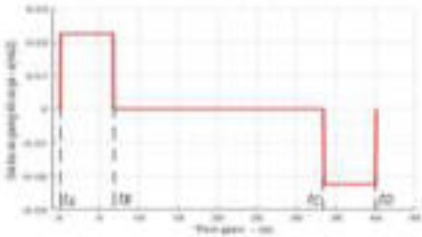

Figure 3.11. Acceleration of the cart when moving forward during the process of cutting wood

Figure 3.9 shows the position error between the input value and the actual position of the carriage over time, the result shows that the largest position error is 0.02 (*m*) corresponding to 20 (*mm*); (Figure 3.10) shows the change in the actual carriage velocity compared to the set velocity over time. (Figure 3.11) shows the actual carriage acceleration achieved and (Figure 3.12) shows the traction force of the transmission system that must be generated to act on the carriage to help the carriage move over time at the desired positions .

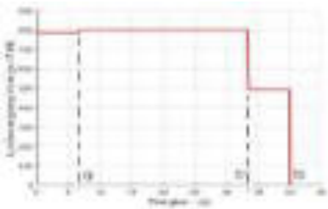

Figure 3.12. The necessary force acting on the cart during the process of moving forward to saw wood.

3.4.2.2. Simulation with the case of the saw moving backwards without cutting wood

The simulation results of the process of the carriage moving backwards without cutting wood are shown in the figures from (Figure 3.13 to Figure 3.15). Figure 3.13 shows the variation in the *x coordinate* of the carriage; Figure 3.14 shows the position error between the input value and the actual position of the carriage over time, the largest error is ~ 20 (*mm*); Figure 3.15 shows the variation in the actual carriage speed compared to the set speed over time .

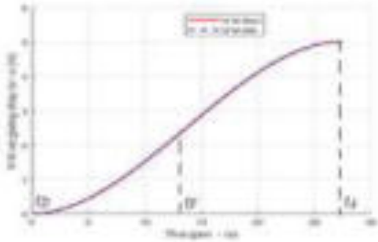

Figure 3.13. Reverse cart movement mode when not cutting wood

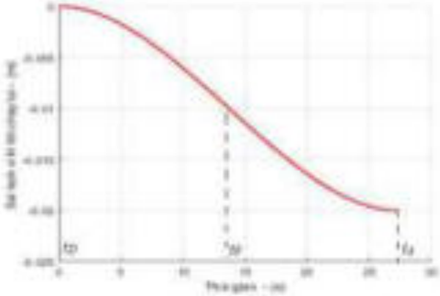

Figure 3.14. Positional deviation when the carriage moves in reverse without cutting wood

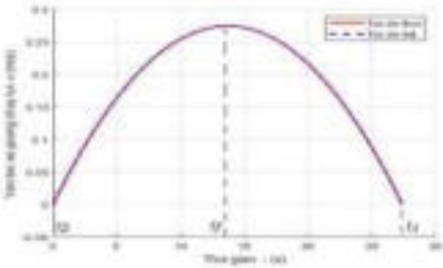

Figure 3.15. The speed of the cart when moving backwards without cutting wood

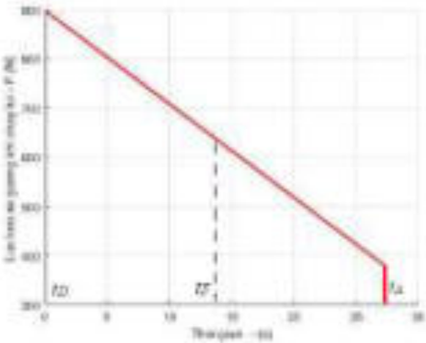

Figure 3.16. Required force acting on the carriage during reverse operation without cutting

3.4.3. Evaluation of dynamic model and controller through simulation results

From the simulation results in two cases of the cart moving forward to cut wood and the cart moving backward without cutting wood, the thesis found that there is a certain deviation in the trajectory between the actual value and the input value of the control system (PD compensates for friction), clearly shown in (Figure 3.9 and Figure 3.14). This deviation occurs greatly starting at the times when there is a change in speed (*point B and point D for moving forward, at this time the speed changes from a uniformly fast motion after a constant velocity motion, and changes from a uniform velocity to a uniformly slow velocity; at point F for moving backward, at this time the speed changes from a uniformly fast motion to a uniformly slow motion*); the maximum deviation of the system in both cases reaches a value of approximately ~20 *mm;* At the same time, static deviation also occurs at the end of the trajectory when the carriage stops, which causes the carriage to not stop correctly at point D when the carriage moves forward (*stops at point* D + 20 (*mm)*) and point E when the carriage moves backward (*stops at point E + 10 (mm)*).

From the survey process during the research, the thesis found that the cause of the trajectory deviation was due to the system's inertia being too large, the mass of the carriage with wood m = 6500 *kg* , causing very large inertia when there was a change in the velocity of the mechanical system.

To overcome this deviation, the thesis proposes to add a brake system installed on the carriage to help the system controller have additional tools to support stopping and adjusting the carriage speed as desired, while helping the quality of the sawing circuit to be faster when the control system closely follows the set trajectory (which is the desired trajectory according to the requirements of sawing technology).

3.5. Investigate the influence of brake cable reverse acceleration and brake cable diameter on the value of braking distance and braking force.

As explained in the first part of section 2.4.1, when calculating the braking force, we will *not take into account the participation of the saw blade resistance force* in the braking process of the carriage.

In fact, the operating speed of the carriage is between 5 – 15 m/min, that is, between 0.085 – 0.25 m/s. Therefore, here we calculate for the case of the carriage braking at maximum speed: *v = 0.25 m/s.*

From formula (2.141), we see that the required braking force is proportional to the length of the segment Δx_2. From (2.139), we see that Δx_2 it increases when the mass *m* and v *are 0.* increases. Therefore, we calculate the braking force required for the case where the carriage mass *m* is the largest and moves at the largest possible speed v *0. In order to be able to choose the diameter* *Φ (mm)* of the brake cable as well as the reverse acceleration of the brake cable a_k *(m/s²)* during the braking process to suit the requirement that *the braking distance* (the distance traveled by the carriage from the start of braking until it stops completely) is within the allowable limit, we conduct a survey of the equations from (2.106) to (2.141) with the parameters given above (Table 3.5).

Table 3.5 4used in the carriage brake investigation

Parameters	Unit	Value	Note
m	*kg*	**6500**	Vehicle weight + wood
E	N/m^2	$2.5*10^9$	Brake cable elastic modulus

λ		0.0033	Self-stretch coefficient of brake cable
L_0	*m*	7	Length of cable section starting to pull the brake
v_0	*m/s*	**0.25**	Speed of the carriage when the brakes are applied
k_{ms}		0.001	Rolling friction coefficient
g	m/s^2	9.81	Acceleration of gravity
a_k	m/s^2	4 ÷ 22	Brake cable reverse acceleration
F	*mm*	10 ÷ 28	Brake cable diameter

Table 3.6 5distance (mm), corresponding to each pair of values Φ and a $_k$

Brake reverse acceleration a_k (m/s^2)	***Brake cable diameter - Φ*** *(mm)*									
	10	**12**	**14**	**16**	**18**	**20**	**22**	**24**	**26**	**28**
4	75	66	60	55	52	48	46	44	42	40
6	67	60	54	50	46	44	41	39	38	36
8	62	55	50	46	43	40	38	36	35	33
10	58	52	47	43	40	38	36	34	33	31
12	55	49	44	41	38	36	34	32	31	30
14	52	47	42	39	36	34	32	31	30	***28***
16	50	45	41	38	35	33	31	30	***28***	***27***
18	48	43	39	36	34	32	30	***29***	***27***	***26***
20	47	42	38	35	33	31	***29***	***28***	***26***	***25***
22	46	41	37	34	32	30	***28***	***27***	***26***	***25***

Table 3.7 6Brake traction force value (N) corresponding to each pair of values Φ and a $_k$

a_k (m/s^2)	***T*** *(mm)*									
	10	**12**	**14**	**16**	**18**	**20**	**22**	**24**	**26**	**28**
4	1659	2055	2458	2867	3280	3696	4116	4538	4962	5388
6	1487	1845	2211	2582	2957	3336	3718	4103	4490	4879
8	1373	1705	2045	2390	2739	3093	3449	3808	4169	4532
10	1289	1602	1922	2248	2578	2912	3249	3588	3930	4274
12	1223	1521	1826	2137	2452	2770	3092	3416	3742	4071
14	1170	1456	1748	2046	2349	2654	2963	3275	3589	***3904***
16	1125	1401	1683	1970	2262	2557	2856	3157	***3460***	*3765*
18	1087	1354	1627	1905	2188	2474	2763	***3055***	***3349***	***3645***
20	1054	1313	1578	1849	2123	2402	***2683***	***2967***	***3253***	***3540***
22	1025	1277	1535	1799	2066	2338	*2612*	***2888***	***3167***	***3448***

Suppose the wood sawing system requires the carriage braking distance not to exceed 30 mm, if the brake cable has the values E and λ as in (Table 3.5), then based on (Table 3.6), we must choose the diameter of the brake cable Φ ≥ 22 mm and design the brake system to achieve the acceleration a $_k$ corresponding to Φ above (Table 3.6) and the corresponding traction force above (Table 3.7). For example, if Φ = 22 mm, the brake system must achieve the acceleration $a_k \geq 20$ m/s ^{2} and the braking force F ≥ 2683 N.

Chapter 3 Conclusion

1. The results of the survey of the horizontal oscillation equation of the saw blade plane have given (Table 3.2) a pair of values (*EI, k*) corresponding to the maximum horizontal oscillation amplitude of the saw blade. This allows for a reasonable selection of the pair of values of the two above parameters during the foundation processing and rail installation in the saw blade production line system to satisfy the condition that the maximum horizontal oscillation amplitude of the saw blade is within the allowable limit.

2. From the survey results in the graphs Figure 3.4 and Figure 3.5 with (Table 3.2), for the horizontal oscillation amplitude to be within the allowable value, the filling depth h_b of the concrete layer of the carriage track foundation will depend on the concrete grade and the ground coefficient k_d (under the concrete layer): When $k_d = 8\ KN/m^3$, concrete grade M300, the thickness of the concrete layer poured for the automatic wood sawing carriage track foundation is $h_b = 0.88\ m$; When $k_d = 14\ KN/m^3$, concrete grade M300, the thickness of the concrete layer poured for the automatic wood sawing carriage track foundation is $h_b = 0.7\ m$.

3. If the distance between the two rails increases, the amplitude of oscillation of angle φ will be smaller, leading to the horizontal oscillation amplitude of the slit track will be smaller. The maximum horizontal oscillation amplitude of the slit track will increase almost linearly with the speed when the carriage speed is in the range $v = 0.03 - 0.07\ m/s$ and almost unchanged when the carriage speed is in the range $v = 0.07 - 0.2\ m/s$.

4. The survey results on carriage braking have provided lookup tables on the relationship between the braking distance and the parameters of the brake cable diameter Φ and the braking acceleration a_k (Tables 3.6; Table 3.7). From the survey results, the parameters for carriage braking are determined as follows: If the diameter of the carriage braking cable is $\Phi = 22\ mm$, the braking system must achieve a traction acceleration $a_k \geq 20\ m/s^2$ and a braking force $F \geq 2683$ N.

CHAPTER 4
EXPERIMENTAL DETERMINATION OF SOME PARAMETERS AND VERIFICATION
THEORETICAL CALCULATION MODEL

4.1. Objectives and objects of experimental research

The thesis conducts experimental research because it is necessary to have experimental research results to compare with the calculation results according to the theoretical model, from which the practical suitability of the theoretical calculation model that has been built can be assessed.

Based on the above reasons, the thesis conducts experimental research with the following objectives and tasks:

4.1.1. Objectives of experimental research

- Experiment to give the values of some parameters: foundation coefficient k_0, self-expansion coefficient of traction cable and brake cable.
- Through experimental data, determine the amplitude of wood sawing oscillation; compare the results obtained with the results calculated through theoretical models and draw conclusions.

- From the experimental results, evaluate the reliability of the established calculation model.

4.1.2. Experimental research subjects

The experimental research object is the automatic wood sawing system by the state-level project " Research, design, manufacture of automatic wood sawing equipment line with capacity of 3-4 m3/h of finished wood " code DTĐL.CN-10/16 has designed and manufactured an automatic wood sawing line. The experimental location is at Vietnam Specialized Equipment Joint Stock Company.

experimental parameters

4.2.1. Select the research objective function

For the wood sawing system to work effectively, the amplitude of sawing circuit oscillation must only be within the allowable limit. Therefore, one of the experimental research objectives of the thesis is ***the amplitude of sawing circuit oscillation*** in the automatic wood sawing system using vertical band saw.

The thesis also chooses the experimental research target of the carriage braking system. Although the carriage runs at a low speed, but because the carriage runs on the rail and has a large mass, the inertia force will make the carriage move with ***a distance*** Δx ***after braking*** . The experiment is to verify: with the design parameters and installation of the foundation system and the carriage, Δx does it meet the requirement of less than the allowable travel distance of the carriage after braking?

4.2.2. Select parameters that affect the objective function

The concrete foundation coefficient k_0 depends not only on the concrete grade but also on the depth, horizontal and vertical width of the foundation, so it is necessary to measure directly by the method: ***Field compression table test*** according to TCVN 9354:2012.

Because the carriage brake cable is a multi-strand cable braided together according to the cable strands, there is always a self-stretch of the cable, that is, before the phenomenon of cable stretching occurs according to Huc's law (due to the stress not appearing in the cable strands), the cable is stretched due to being stretched (under the effect of tensile force); the stretched cable section ΔL (due to the cable being stretched) will be proportional to the initial cable length L_0 according to the self-stretch coefficient λ , that is:

$$\lambda = \frac{\Delta L}{L_0} \qquad (4.1)$$

Summary : In this thesis, some parameters are selected for experimental measurement, which are the foundation coefficient k_0 and the cable self-expansion coefficient λ. These are parameters that must be known when installing the sawing line, so they need to be calculated accurately so that the oscillation amplitude of the wood sawing circuit is within the allowable limit when the sawing line system is operating .

4.3. Experimental method for determining the foundation coefficient k_0 and the cable self-expansion coefficient λ

4.3.1. Experimental determination of the foundation coefficient k_0

Soil compression table tests are performed at designated locations to find out the actual settlement of the foundation under given loads.

Formula for determining the background coefficient k_0: $$k_0 = \frac{p_2 - p_1}{s_2 - s_1}$$ (4.2)

in which: p_1, p_2 is the experimental compression pressure level with corresponding settlement s_1, s_2.

4.3.1.1. Field compression table testing process

+ **Loading process** :

Loading according to 10 pressure levels (0.0 – 0.06 – 0.12 – 0.18 – 0.24 – 0.3 – 0.36 – 0.42 – 0.48 – 0.54 – 0.6 kg/cm2). In each loading level, record the position of point B' on the screen to calculate the distances BB' for each time. The load holding time of each loading level and allocated to record point B' on the screen: 10 minutes - 10 minutes - 10 minutes - 15 minutes - 15 minutes - 30 minutes - 30 minutes - 30 minutes - 30 minutes. Deloading is also according to 10 levels. The deloading time of each level is 30 minutes and is allocated to record the meter reading as follows: 10 minutes - 10 minutes - 10 minutes.

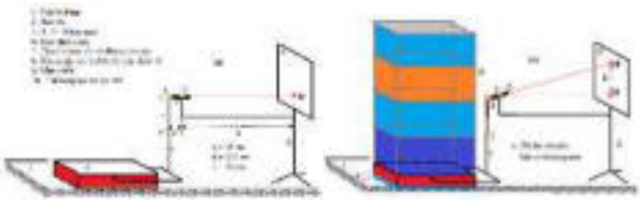

Figure 4.1 1Description of experimental equipment for field compression table using static loading

(a)- When the compression table is not loaded yet; (b)-When the compression table is loaded;

4.3.1.2. Processing experimental measurement results

The measured data during the loading process at 10 levels are recorded in (Table 4.1) in columns (1) and (2). The description of the calculation of the foundation coefficient k_0 according to the experimental measurement arrangement is presented above (Figure 4.2).

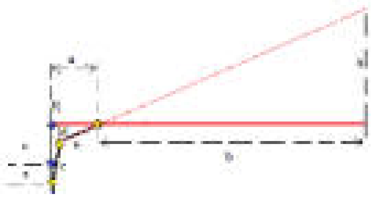

Figure 4.2 2Model for calculating the background coefficient k $_0$ according to the experimental measurement layout

With the arrangement of experimental equipment leading to the above calculation model (Figure 4.2) we get the formulas: Set $\frac{h}{b} = u$ => $x = a\left(1 - \frac{1}{\sqrt{1+u^2}}\right)$; $d = \frac{au}{\sqrt{1+u^2}}$

=> settlement $s = \sqrt{c^2 - x^2} + d - c$, with a = c = 10 cm, b = 200 cm

Table 4.1 1Results and data processing of the compression table loading process

Compressive pressure p (N/m ^{2})	h(mm)	u	x(m)	d (m)	s (m)	k $_0$ (N/m ^{3})	k $_0$ - step (N/m ^{3})
(1)	(2)	(3)	(4)	(5)	(6)	(7)	(8)
0	0	0	0	0	0	0	0
6000	5	0.025	3.1E-06	2.5E-04	2.5E-04	2.4E+07	2.4E+07
12000	11	0.055	1.5E-05	5.5E-04	5.5E-04	2.2E+07	2.0E+07
18000	16	0.08	3.2E-05	8.0E-04	8.0E-04	2.3E+07	2.4E+07
24000	22	0.11	6.0E-05	1.1E-03	1.1E-03	2.2E+07	2.0E+07
30000	28	0.14	9.7E-05	1.4E-03	1.4E-03	2.2E+07	2.0E+07
36000	33	0.165	1.3E-04	1.6E-03	1.6E-03	2.2E+07	2.5E+07
42000	40	0.2	1.9E-04	2.0E-03	2.0E-03	2.1E+07	1.8E+07
48000	46	0.23	2.5E-04	2.2E-03	2.2E-03	2.1E+07	2.1E+07
54000	53	0.265	3.3E-04	2.6E-03	2.6E-03	2.1E+07	1.9E+07
60000	60	0.3	4.2E-04	2.9E-03	2.9E-03	2.1E+07	1.9E+07

From the measured data, the quantities *u, x, d, s* are calculated, recorded in columns (3) - (6) in Table 4.1.

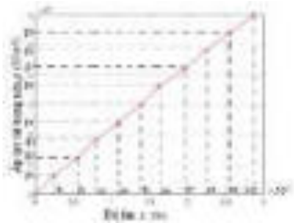

Figure 4.3 3Graph of the relationship between compressive load pressure and compression table settlement

Figure 4.3 describes the relationship between the pressure of the compressive load and the corresponding settlement (recorded in columns (1) and (6) of Table 4.1).

On Table 4.1:

+ Column (7) records the result of calculating the background coefficient calculated according to the formula: $k_0^{(i)} = \frac{p_i}{s_i};\ i = 1 \div 10$ (4.3)

+ Column (8) records the result of calculating the background coefficient calculated according to the formula

$$k_0^{(i)} = \frac{p_i - p_{i-1}}{s_i - s_{i-1}}\ ;\ i = 1 \div 10\ ;\ s_0 = 0 \qquad (4.4)$$

Formula (4.3) shows the foundation coefficient k_0 calculated according to the total pressure and the total settlement respectively; formula (4.4) shows the foundation coefficient k_0 calculated according to the loading value and the increase of the settlement respectively.

Therefore, we can take the average value: $k_0 = \frac{1}{10}\sum_{i=1}^{10} k_0^{(i)} \approx 21.10^6 \left(N/m^3\right)$

(4.5)

4.3.2. Experimental determination of self-expanding cable coefficient λ

4.3.2.1. Experimental process to determine the self-expanding cable coefficient λ

+ Experimental setup

One end of the cable is connected to the fixed force meter, the other end of the cable is connected to the cable winch. The cable is placed straight on a flat surface and in a free state; Call A the connection point of the cable and the force meter, mark point B (on the cable) so that the length AB = 10 m.

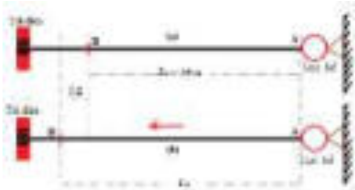

Figure 4.5 4Experimental layout to determine the self-expanding cable coefficient λ

(a)– Cable section in free state;

(b)- The cable is pulled until stress appears in the cable.

Control the electric winch to slowly pull the cable until the dynamometer shows the tensile stress value of the cable, at this time point B will be at position B'. Measure the length AB' by L_d, get: $\Delta L = L_d - L_0 \Rightarrow \lambda_i = \frac{\Delta L}{L_0}$

Table 4.2 2Experimental measurement results for calculating the brake cable self-expansion coefficient

TT	$L_0 (m)$	$L_d (m)$	$\Delta L (m)$	λ_i
1	10	10.05	0.05	0.005
2	11	11.06	0.06	0.0055
3	9	9.02	0.02	0.0022
4	10	10.03	0.03	0.003
5	10.4	10.45	0.05	0.0048
6	10	10.05	0.05	0.005
7	11.5	11.53	0.03	0.0026
8	10.5	10.52	0.02	0.0019
9	9.5	9.51	0.01	0.0011
10	11	11.02	0.02	0.0018

The above measurement experiment was performed on 10 different cable sections, the results are recorded above (Table 4.2). The self-expansion coefficient of the cable is calculated based on the average value of the measurements:

$$\lambda = \frac{1}{10}\sum_{i=1}^{10} \lambda_i \qquad (4.6)$$

From the results of the measurements recorded above (Table 4.2), the self-expansion coefficient of the brake cable is obtained according to (4.6): λ = 0.0033

(4.7)

4.4. Experimental measurement of horizontal vibration amplitude of wood sawn joints

This measurement result is compared with the calculation result at point M according to the theoretical model.

Three points A, B and M are on the carriage and on a straight line parallel to the rails. At A and B, sensors measuring horizontal acceleration are placed.

From the measurement results of the horizontal oscillation amplitude at two points A and B, we can calculate the oscillation amplitude at point M by the following calculation:

Let the distance AB be d_{AB}, the distance AM be $x = x_0 + vt$. Here x_0 is the initial distance when the cart has not yet moved, v (*m/s*) is the velocity of the cart, *t (s)* is the time in seconds. Choose the coordinate system as shown in the figure, then the *y coordinate* $_M$ in the horizontal direction of point M is calculated:

$$y_M = \frac{x}{d_{AB}}\left(y_B - y_A\right) + y_A \qquad (4.8)$$

in which: y_A and y_B are the horizontal coordinates of points A and B.

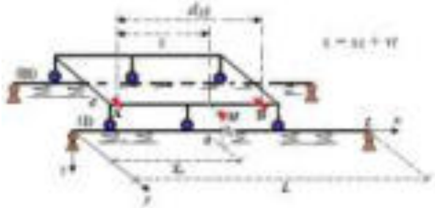

Figure 4.6 5Diagram of placing horizontal acceleration sensors at points A and B at the same height as M on the carriage.

4.4.1. Measuring equipment used in experimental research

a) DMC-Plus signal amplifier

The thesis uses the DMC-Plus signal amplifier of the Federal Republic of Germany. This device is a device that collects and amplifies measurement information connected to a computer as shown in Figure 4.6. This device replaces the K amplifier and the A/D (Analog/Digital) converter in the schematic diagram of the experimental method. The DMCPlus device has modules manufactured according to the following channels:

+ DV01 module: DC current amplifier module, used to measure temperature, connected to thermocouples, DC currents. This module can measure voltage sources with a very wide measuring range (±0.1V; ±1V; ±10V; ±200V), frequency range 2.2 kHz.

+ DV10 module: DC current amplifier type, to connect full and half resistor bridges, can measure voltage, DC voltage source, frequency range 4.4 Hz.

+ DV30 module: Amplifier type is 600Hz frequency, used to measure full and half bridge resistors, measure voltage, DC voltage source, frequency range 250 Hz.

+ DV35 module: Frequency amplifier type, suitable for measuring resistance, DC voltage source, frequency range 250 Hz.

+ DV55 module: The amplification type is frequency, the amplification range is 4.8 kHz, very popular. Used to connect to full and half resistor bridges, measure voltage of DC voltage sources, frequency range 2.2 kHz.

+ Module DZ65: Used to connect sensors measuring torque, speed and power.

Figure 4.7 6DMC Plus device

b) Accelerometer sensor B12/1000

To determine the horizontal acceleration of the carriage when moving during the sawing process, the thesis uses an inductive acceleration probe manufactured by HBM of the Federal Republic of Germany. The shape and schematic diagram are shown in Figure 4.8.

Figure 4.8 7Accelerometer B12/1000

1- Inertial mass; 2 - Cross section of two inductance coils; 3 - Leaf spring (elastic element); 4 - Probe body; 5 - Chamfered edge; 6 - Wire connection post; 7 - Threaded end mounted on the measured object

The sensor is fixed at a determined position on the carriage horizontally. When the carriage oscillates horizontally, it will cause the inertial mass (1) to oscillate in the two inductance coils (2), causing the magnetic reluctance of the magnetic circuit to change, leading to a change in the inductance of the two coils (2).

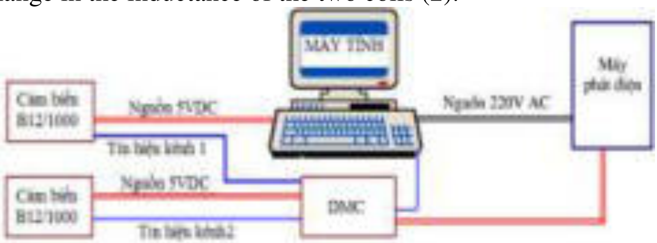

Figure 4.9 8Connection diagram of measuring device with measuring sensor

4.4.2. Method of processing experimental results

a) Number of measurement data

Because the population is not known, **the sample size** will be determined using the formula: $N = Z^2 \dfrac{p(1-p)}{e^2}$ (4.9)

From (4.9) we get the minimum amount of measurement data:

$N = 1.96^2 \dfrac{0.5(1-0.5)}{0.05^2} = 384.16$ (4.10)

To verify the theoretical calculation model on experimental measurement data, the horizontal acceleration of the carriage when moving on the rail is measured. Because the distance the carriage moves on the rail during the wood cutting process is 6 m, the moving speed of the carriage v = 0.15 m/s, the carriage moves the entire wood cutting distance with a time of T = 40 s. The measuring device is set to measure every 0.1 s, resulting in the number of measurement data on each sawing circuit $N = 400 > 384,16$ satisfying the condition of the number of measurement data (4.10).

b). Method for calculating the amplitude of horizontal oscillation of the carriage (at the point where the measuring sensor is placed) from experimental data of acceleration measurement.

Through the experiment*, the data received is the lateral oscillation acceleration of the vehicle at the measurement point. The value of the lateral oscillation amplitude at the measurement point will be calculated according to the following method:*

+ Let T (s) be the time interval from the start of the acceleration measurement to the end, with the measurement time step being Δ t. Thus, we will have the number of measurements M: $M = \frac{T}{\Delta t} + 1$ (4.11)

+ Acceleration measurements $\ddot{y}$ are represented as a Fourier series with only cosines with $N+1$ terms:

$$\ddot{y}(t) \approx \frac{a_0}{2} + \sum_{k=1}^{N} a_k \cos\left(\frac{k\pi}{T} t\right) \tag{4.13}$$

The integration (4.13) together with the conditions $\omega(0) = 0;\ \dot{\omega}(0) = 0$ leads to a function representing the angular amplitude from the measured data:

$$y(t) \approx \frac{a_0 t^2}{4} - \sum_{k=1}^{N} a_k \frac{T^2}{(k\pi)^2} \cos\left(\frac{k\pi}{T} t\right) + \sum_{k=1}^{N} a_k \frac{T^2}{(k\pi)^2} \tag{4.16}$$

Note that, since the Fourier series converges slowly, the number of terms N in the sum (4.16) is quite large. In the thesis, the calculation is with $N=290$.

c). Check the correlation between two sets of values

The correlation coefficient (r) is a statistical index that measures the correlation relationship between two variables x and y . The correlation coefficient has a value from -1 to 1. A correlation coefficient of 0 (or close to 0) means that the two variables have no relationship to each other; conversely, if the coefficient is -1 or 1, it means that the two variables have an absolute relationship. If the value of the correlation coefficient is negative (r <0), it means that when x increases, y decreases (and vice versa, when x decreases, y increases); if the value of the correlation coefficient is positive (r > 0), it means that when x increases, y also increases, and when x *decreases* , y also decreases.

There are many correlation coefficients in statistics: Pearson correlation coefficient r , Spearman ρ, Kendall τ. In this thesis, Pearson correlation coefficient *r is used* to evaluate the correlation between the series of angular acceleration values obtained through measurements and from its regression function. Pearson correlation coefficient r is also used to evaluate the correlation between the series of angular amplitude values obtained from the experimental regression function (through angular acceleration measurement data), with the series of values obtained from the calculation model; in this case, if the correlation coefficient $r \geq 0.8$ then the calculation model built in the thesis can be accepted.

4.4.3 Organization of the experiment

c) Parameters of the wood sawing system

Table 4.3 3Parameters used during the survey

Symbol	Content	Value
d_1	Distance between middle and top wheel axles	2.5 [m]
d_2	Distance between last and first wheel axle	6.5 [m]
d	Distance between two rails	1.5 [m]
v	Speed of the cart (speed of pushing the log)	0.15 [m/s]
L	Length of rail beam	15 [m]
b	Width of the rail beam	0.1 [m]
k_0	Rail foundation coefficient	21x106 [N/m^3]
b_c	Width of vertical circular saw tooth set	2.5 [mm]
n_c	Teeth per inch (TPI) (or 0.0254 m)	4
L_{cut}	Wood cutting length	20 [inches] (or 0.508 m)
n_{cr}	Number of saw blade teeth in cutting circuit	$n_{cr} = n_c L_{cut}$
ω_c	Saw wheel rotation speed	700 [rpm]
D	Saw wheel diameter	38 [inches] (or 0.965 m)
K	Specific shear resistance	36.15 [N/mm ^{2}]
ρ	Mass per unit length of track	40 [kg/m]
X_c	x coordinate of vertical band saw blade	3 [m]
u	Y coordinate of saw blade cutting point	0.5 [m]
h	The height of the point calculates the horizontal amplitude of the wood cutting line.	1.2 [m]

The experiment was carried out on an automatic wood cutting system using a vertical band saw with the parameters recorded in (Table 4.3).

d) Conduct the experiment

When the installation work is completed, the thesis conducts the following experiments:

- Let the sawing system operate, the carriage speed gradually increases and stabilizes at 9 m/min (ie 0.15 m/s).

- When the vehicle moves to position M marked with distance AM equal to x_0, start recording acceleration measurement data at A and B.

The experimental setup and organization are shown in (Figure 4.11 and Figure 4.12).

Figure 4.10 9Experimental setup for measuring the amplitude of horizontal oscillation of the slit circuit

Figure 4.11 10Oscillation acceleration measurement process carriage

The horizontal oscillation acceleration graph at point A during the sawing process is recorded in the form of a graph shown in Figure 4.12.

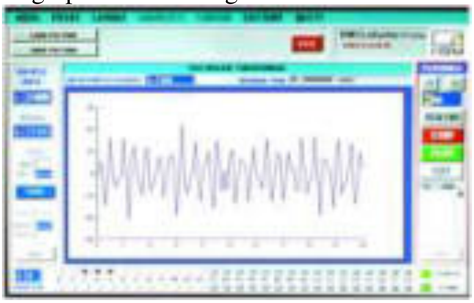

Figure 4.12 11Horizontal oscillation acceleration graph at point A during the cutting process.

4.4.4. Process measured data and compare experimental results with calculated results according to theoretical models.

The experimental results were obtained in the form of a chart (Figure 4.13) and in the form of numbers over time with a recording step of 0.1s, and were recorded on EXCEL. The data are shown in the appendix above (Table 3).

On the graphs in Figure 4.13: The measured acceleration data are shown by the red '*' signs. Based on these measured data, calculated according to the empirical regression function of the form (4.13) with the number of terms N = 175 and N = 290, the acceleration regression function results are shown in Figure (4.13).

The acceleration regression function according to (4.13) is of the form: $\dot{y}(t) \approx \frac{a_0}{2} + \sum_{k=1}^{N} a_k \cos\left(\frac{k\pi}{T} t\right)$

In which the coefficients a $_0$ and a $_k$ ($k = \overline{1 \div N = 290}$) are recorded in (Appendix Table 2). When obtaining the experimental regression function of the acceleration measurements, we can integrate twice to obtain the experimental regression function of the oscillation amplitude according to formula (4.16):

$$y(t) \approx \frac{a_0 t^2}{4} - \sum_{k=1}^{N} a_k \frac{T^2}{(k\pi)^2} \cos\left(\frac{k\pi}{T} t\right) + \sum_{k=1}^{N} a_k \frac{T^2}{(k\pi)^2}$$

The experimental regression graph of the amplitude is shown by the red line above (Figure 4.14). Compare it with the value of the oscillation amplitude calculated from the theoretical model of the blue line above (Figure 4.14). It is seen that the larger the number of terms N, the more accurate the regression function will be. Therefore, the calculations here will take N = 290.

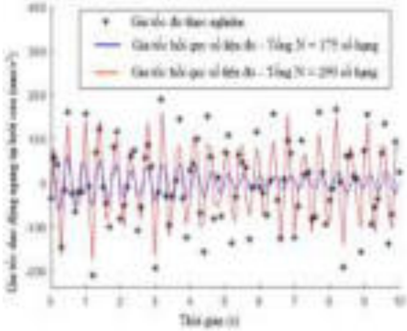

Figure 4.13 12Graph of experimental measured values and regression of horizontal oscillation acceleration of the saw blade at the point where the saw blade cuts the wood:

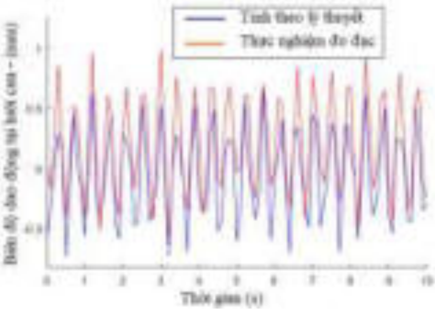

Figure 4.14 13Graph comparing experimental results with the model for calculating the amplitude of sawing vibration during the sawing process.

The values of the amplitude of horizontal oscillation of sawn joints over time during the sawing process, calculated according to the theoretical model and experimental measurements, are recorded in (Table 1 of the appendix) in columns 4 and 5. Comparing the correlation of these two series of numbers over time t gives a correlation coefficient of r ≈ 0.89. This proves that the theoretical calculation model used in the thesis is close to reality.

CONCLUSION OF CHAPTER 4

1. An experimental research method has been established to indirectly determine the amplitude of oscillation of the wood sawn surface through experimental measurements of horizontal oscillation acceleration at two different points on the carriage, thereby selecting measuring devices, sensors, and methods for processing experimental data.

2. From the experimental results of determining the horizontal oscillation amplitude of the saw blade compared with the oscillation amplitude obtained from the theoretical calculation model, it can be seen that: the series of these values all have a correlation coefficient $r > 0.8$. That proves that the theoretical calculation model is consistent with reality and is reliable .

CONCLUSION AND RECOMMENDATIONS

1. Conclusion

Based on the results of theoretical and experimental research on the dynamics and control of carriages in automatic wood sawing lines using vertical band saws, the thesis has achieved the following results:

1. Build a model and establish dynamic equations for the longitudinal motion of an automatic wood sawing cart. Based on the established dynamic model, the thesis has built a longitudinal motion control algorithm and a carriage braking control algorithm.

2. The thesis has built a model for calculating the horizontal oscillation of the plane of the sawn timber, the problem is converted to the oscillation of the beam on an elastic foundation, subjected to many concentrated loads that change and move. By using the properties of the Dirac function, the thesis has established the equation of the horizontal oscillation of the sawn timber and given the solution in analytical form. From the results obtained, the expressions for the natural oscillation frequency and the forced oscillation frequency allow to conclude: With the sawn timber chain systems using vertical band saws and automatic sawn timber carriages, the resonance phenomenon of the beam rail does not occur.

3. The thesis has investigated the horizontal oscillation equation of the sawn joint and given the results (Table 3.2), which shows the pairs of values of the bending stiffness of the rail beam EI and the foundation coefficient $k = k_0.b$ corresponding to the horizontal oscillation amplitude of the carriage reaching the maximum value. Based on this result, a reasonable choice can be made: the parameters of EI and k_0 as well as the thickness h_b of the concrete foundation layer serving the construction process when installing the carriage foundation, ensuring that the maximum horizontal oscillation amplitude of the sawn joint plane is smaller than the allowable limit. For example, with $EI = 75.10^6$, the limit of the width of the sawn joint $b_{gh\text{-}m} = 1\ mm$: When $k_d = 8\ KN/m^3$, concrete grade M300, the thickness of the concrete layer $h_b = 0.88\ m$; When $k_d = 14\ KN/m^3$, concrete grade M300, then concrete layer thickness $h_b = 0.7\ m$.

4. The thesis has built a model, established the dynamic equation of the carriage braking process, the results of the survey of the dynamic equation of the carriage braking, and provided a table of parameters for the carriage braking, ensuring that the braking distance is less than the allowable distance. For example, if the carriage braking distance *does not exceed 30 mm,* with the diameter of the carriage braking cable $\Phi = 22\ mm$, the braking system must achieve a traction acceleration $a_k \geq 20\ m/s^2$ and a braking force $F \geq 2683$ N.

5. The thesis has established a method for experimentally studying the dynamics and control of carriages in an automatic wood sawing line. Experiments have been conducted to determine the foundation coefficient and the self-expansion coefficient of the carriage brake cable. Measurement of the horizontal oscillation amplitude of the sawing joint is conducted indirectly by measuring the horizontal acceleration at two different points on the carriage. Experimental results to verify the theoretical calculation model of the horizontal oscillation of the sawing joint show that the correlation coefficient r between the series of oscillation amplitude values of the theoretical calculation model and the experimental results all satisfy $r > 0.8$; that proves that the theoretical calculation model is consistent with reality.

2. Recommendations

Due to time and research scope constraints, to complete the study on the dynamics and control of carriages in the wood sawing line, it is necessary to continue studying the following contents:

1. Research to determine some optimal parameters of the carriage in the automatic wood sawing line to meet the requirements of improving productivity, quality and safety during operation.

2. Build and set up an optimal control system for the carriage in the automatic wood sawing line to improve productivity, quality and safety for the carriage system in the automatic wood sawing line.